Energy Conversion and Management: X 26 (2025) 101027

Contents lists available at ScienceDirect

Energy Conversion and Management: X

journal homepage: www.sciencedirect.com/journal/energy-conversion-and-management-x

A novel energy management system based on two-level hierarchical economic model predictive control for use in microgrid control

F.J. Vivas [b,*], A. Pajares [a], X. Blasco [a], J.M. Herrero [a], F. Segura [b], J.M. Andújar [b]

[a] Instituto Universitario de Automática e Informática Industrial, Universitat Politècnica de València, Valencia, Spain
[b] Research Centre on Technology, Energy and Sustainability (CITES), University of Huelva, Spain

ARTICLE INFO

Keywords:
Hierarchical control
Optimal control
Model predictive controller
Energy management system
Renewable microgrids
Hydrogen-based store system

ABSTRACT

This study proposes an innovative energy management system (EMS) based on two-level hierarchical model predictive control, designed for microgrid control. MPC-based EMS are economically efficient and beneficial, although the real-time implementation often requires hierarchical structures due to high computational costs. The high level defines a long-term economic optimisation, with a longer sampling period and prediction horizon. Traditionally, the lower level is based on a tracking index of the high-level reference with a shorter sampling period and prediction horizon. In this case, it is necessary to determine the optimisation index weights, a complex selection that depends on the specific characteristics of each microgrid. Generally, the weights are determined by trial and error, lacking a clear physical meaning. Therefore, in this work, a new approach is proposed where the low level performs economic optimisation (similar to high level) in a short-term. Both approaches were evaluated through a practical case in a microgrid. The results obtained show that the traditional tracking approach can generate undesirable effects (unnecessary energy transactions and frequent switching of devices) that produces economic losses, which can only be mitigated by a careful adjustment of the weights. In contrast, the proposed economic approach eliminates these undesirable behaviours, and the need for weight definition, achieving an economic improvement of 3–25%. Therefore, the results confirmed the effectiveness of the proposed new approach, which provides better economic results while overcoming the limitations of traditional tracking methods.

Introduction

Microgrids, particularly those powered by renewable energy, are expected to play a pivotal role in the ongoing energy transition [1,2]. These systems form the foundation of distributed generation, enhancing the efficiency and resilience of the power grid while facilitating the integration of renewable energy sources and emerging technologies that are challenging to implement at scale.

Among the various microgrid architectures, there is growing interest in configurations that incorporate hybrid energy storage systems (HESS). These systems combine battery-based storage system and hydrogen-based storage system (BSS and HBSS, respectively) [3,4]. HESS offers significant advantages in terms of dynamic response and energy capacity, but this comes at the cost of increased control complexity [5,6].

To ensure optimal operation of these complex microgrids, energy management strategies (EMS) are essential [1,6]. To this end, many optimal control techniques exist in the scientific literature, perhaps the most widespread being model-based predictive control (MPC) [7,8]. MPC has emerged as a widely used optimal control technique due to its ability to handle multivariable systems, constraints, and disturbances while predicting future behaviour, an essential feature for managing microgrids [8,9].

The design and implementation of MPC-based EMS for the control and management of renewable and microgrids is well-established in the literature [10,11]. The evolution of these systems, particularly for renewable and hydrogen-based microgrids, has advanced significantly. Early research demonstrated the technical feasibility of MPC-based EMS for simple microgrid architectures. More recent developments focus on designing complex MPC controllers that optimise the economic performance of intricate microgrid systems [12,13]. Current trends emphasize addressing optimal control problems with multiple constraints, cost functions, and a high number of variables to maximize microgrid performance [14,15]. These cost functions account for various operational aspects, including device dynamics, degradation, and associated costs

* Corresponding author.
E-mail address: francisco.vivas@die.uhu.es (F.J. Vivas).

https://doi.org/10.1016/j.ecmx.2025.101027
Received 2 February 2025; Received in revised form 28 March 2025; Accepted 16 April 2025
Available online 30 April 2025

Nomenclature

Acronyms

BoP	Balance of plant
BSS	Battery-based storage system
CAT I	Tracking problems related to the energy or power status of HESS
CAT II	Tracking problems related to the energy and power status of HESS
CAT III	Tracking problems related to the energy and power status of HESS with cost terms included
EMS	Energy management system
ESS	Energy storage system
HBSS	Hydrogen-based storage system
HESS	Hybrid energy storage system
HL	High-level
LHV	Lower heating value
LL	Low-level
LOH	Level of Hydrogen
MEF	Manipulable energy flow
MEG	Main electrical grid
MPC	Model-based predictive control
non-MEF	Non-manipulable energy flow
O&M	Operation and maintenance
PH	Prediction horizon
SOC	State of charge

Symbols

C_i^{var}	Variable cost MEF_i (€/Wh)
C_i^{fix}	Fixed cost MEF_i (€/h)
C_i^{start}	Start cost MEF_i (€)
C_i^{degr}	Degradation cost MEF_i (€/W^2)
CN_i	Energy capacity of element i ($i = \{BSS, HBSS\}$). (Wh)
ESS_j	Energy storage system ($j = \{1, \cdots, n\}$)
ΔP_i	MEF_i power variation (W)
δP_i	MEF_i increment power without on and/or off process (W)
$\eta_{ch/dis}^j$	Charge/discharge efficiency ESS_j (%)
$\overline{H}/\underline{H}$	Maximum and minimum value of variable H (H $= \{x_l, P_i, \Delta P_i\}$)
K_{Pch}/K_{Pdis}	Coef. to BSS related to charge/disc. power (V/W)
K_{SOC}	Coef. to BSS related to SOC (V/%)
$K_{V_{BUS}}$	Coef. to BSS related to V_{BUS}
$Loss$	Total losses of the microgrid (W)
$Loss_i$	Variable losses depending on the power of MEF_i (W)
$Loss_i^{BoP}$	Balance of plant of element MEF_i (W)
n	Number of ESS systems
$\omega_{\delta P_i}$	Weight to penalise power variation
ω_{P_i}	Weight to penalise power tracking error
ω_{Start_i}	Weight to penalise the number of startups
ω_{SOC_j}	Weight to penalise SOC tracking error
MEF_i	Manipulable energy flow ($i = \{ch_1, dis_1, \cdots, ch_n, dis_n, grid_s, grid_p\}$)
P_i	MEF_i power (W)
P_{nMEF-}	Total power non-MEF supplied by the microgrid (W)
P_{nMEF+}	Total power non-MEF injected by the microgrid (W)
P_{EV}	Electric vehicle power (W)
P_{HA}	House appliance power (W)
P_{HVAC}	Heat., vent., and air cond. power (W)
P_i^{ref}	Reference MEF_i power (W)
$PH_{HL/LL}$	Prediction horizon of HL/LL (h)
$r_{ch/dis}^j$	Charge/discharge ratio related to element ESS_j (%/W)
SOC_j	State of charge of ESS_j (%)
SOC_j^{ref}	Reference state of charge of ESS_j (%)
$Start_i$	Start MEF_i (binary)
T_s	Sample time (h)
$Ts_{HL/LL}$	Sample time HL/LL (h)
V_{BUS}	DC bus (and BSS) voltage (V)
WT_i	Working time MEF_i (binary)
$x(k)$	State variable (SOC, LOH, V_{BUS})
v_k	Independent term related to V_{BUS} model (V)

[16–18].

However, the increasing complexity of optimisation problems can make solutions computationally intensive or even unsolvable in real-time applications [19,20]. To mitigate this, hierarchical control structures with MPC controllers operating at different time scales (or levels) have been proposed. The objective is to develop EMS solutions that are computationally efficient while closely approximating the performance of more complex controllers during the short sampling periods required for real-time applications [21,22].

A hierarchical structure for microgrid control typically consists of three levels [23,24]. The primary level operates on a fast time scale and maintains voltage and frequency stability during changes in generation or demand [19,25]. This control is implemented locally. The secondary level ensures that voltage and frequency deviations return to zero after changes in load or generation, eliminating steady-state errors introduced by the primary control [19,25]. Tertiary control manages power flow between the microgrid and external systems, optimizing operations over long time scales for planning and scheduling [25,26]. This level can include various optimisation strategies depending on the time scales involved. The term EMS refers to a system that addresses some of these issues (mainly scheduling and energy sharing) and therefore comprises secondary and tertiary levels. Consequently, this work does not cover control at the primary level. In this paper, the tertiary and secondary levels are referred to as high-level (HL) and low-level (LL), respectively.

The most common two-level solutions use hierarchical MPC with a unidirectional flow of information from HL to LL [24,27]. This structure is computationally efficient and offers proven performance. An example of this controller architecture is depicted in Fig. 1.

This architecture is initially composed of a HL controller, which performs economic optimisation (Economic MPC) over long prediction horizons (PH), spanning hours or days, and employs large sample times to manage high computational cost (typically tens of minutes or hours) [27,28]. However, due to the long sampling intervals, the information available in the HL is biased, as it only provides an average economically optimal schedule. This limitation makes it unsuitable for directly implementing the energy program calculated at this level in the microgrid, as illustrated in Fig. 1. Generally, the MPC controller governing the HL (usually called Day-ahead MPC) incorporates complex objective functions expressed in purely economic terms [17,27]. These objectives are tailored to the microgrid's specific application and architecture, encompassing costs such as energy purchase/sale from the main electrical grid (MEG), operation and maintenance (O&M) costs, and degradation expenses, among others [8,29].

Conversely, the LL MPC executes the control actions on the microgrid based on the optimal energy program calculated by the HL. These actions are applied over shorter PHs and sampling times (on the order of seconds or minutes) [27,28], as illustrated in Fig. 1. Within this two-level framework, it is essential that the LL controller applies a proper control law to implement the HL's optimal energy program, taking into account the differing time scales [16,29]. To address this control

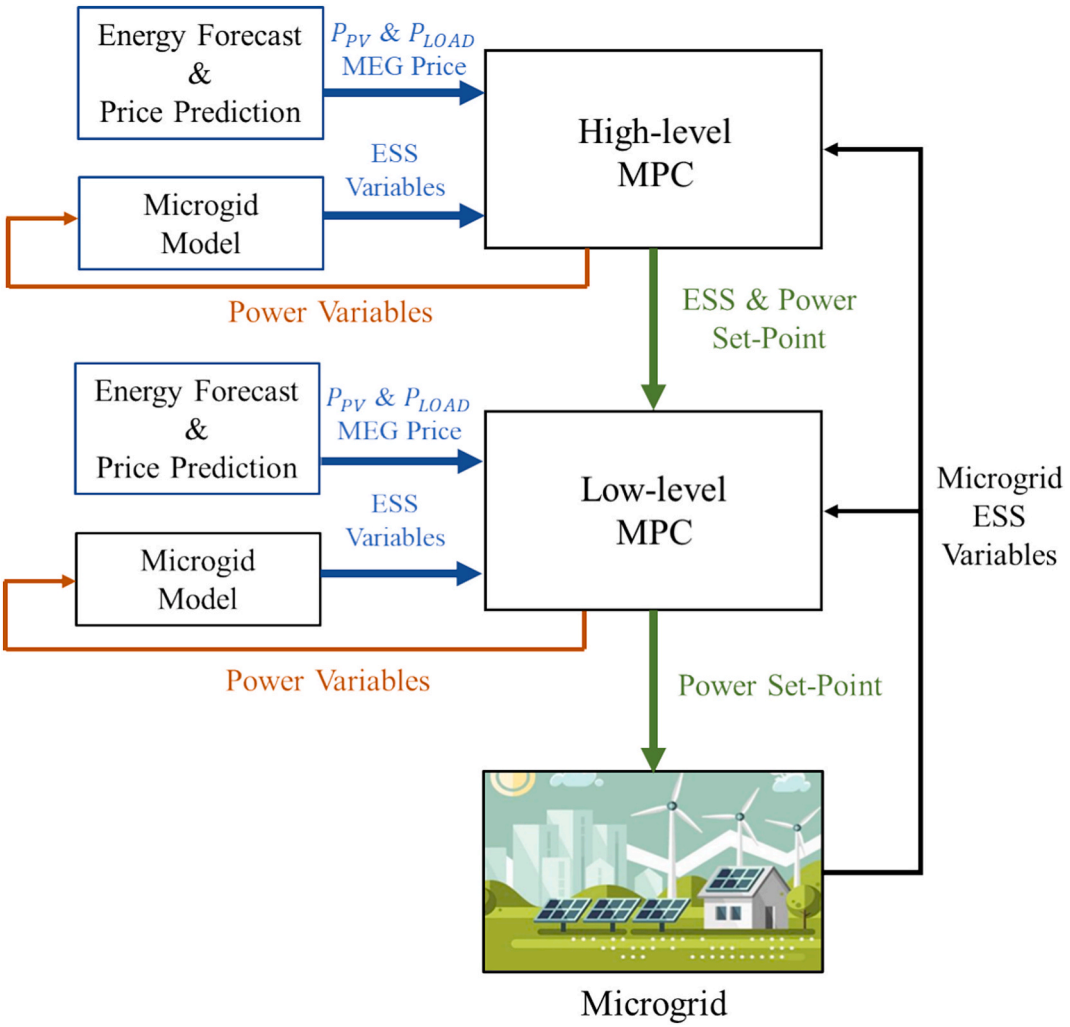

Fig. 1. Two-level hierarchical MPC controller architecture.

requirement, scientific literature offers a wide array of MPC controller solutions. The most common approach, however, is the implementation of MPC controllers designed to solve a tracking problem (Tracking MPC) by following the optimal energy schedule determined by the HL [23,24].

According to the scientific literature, tracking problems can be broadly categorized into three types: HESS energy state or power tracking (CAT I), HESS energy state and power tracking (CAT II) and HESS energy state and power tracking with cost terms included (CAT III).

CAT I type algorithms propose a LL Tracking MPC whose objective function calculates the energy program that ensures tracking of the optimal state of charge (SOC) and level of hydrogen (LOH) values for the HESS, or the power references for the HESS and/or MEG set by the HL. These algorithms define a relatively simple multi-objective problem that does not require weighting factors, as both variables can be normalized to unit values.

CAT I-type algorithm has been successfully applied in two-level MPC-based EMS design with SOC and LOH tracking. These applications include analysing the long-term economic viability of microgrids with electric, thermal, hydrogen, and water loads and services [30]. Generic Tracking MPCs for HESS and MEG power tracking have been used to optimise energy plans for data center power supply [31], residential isolated applications [22], and load frequency control [32]. Similar approaches are described in [17,27] and [28], where Tracking MPC is used for MEG power tracking to optimise the dynamic response and power reserve management of microgrid communities in electricity markets. Additionally, more complex variants implement Tracking MPCs for power and HESS/MEG operating cycle tracking to optimise power flow in microgrid communities offering electricity market flexibility [33,34] and demand-side management services [25].

Despite their advantages, CAT I algorithms have notable drawbacks that may compromise the overall performance of two-level MPC-based EMS. These challenges stem from the problem formulation. While the reference values to be followed are defined, it is important to note that these values represent the optimal average values provided by the HL. Additionally, the requirement is only to reach these references at the end of the PH, not at each sampling period, which is misaligned with the formulation of this type of controller.

Consequently, CAT I algorithms may produce solutions with multiple possibilities and fail to account for crucial factors such as MEG costs or equipment degradation. As a result, the energy schedules determined by CAT I algorithms might not align optimally with HL objectives, and SOC and LOH (and power) reference levels may not be precisely achieved, as the objective function minimizes tracking error but does not guarantee null error.

CAT II algorithms improve upon CAT I by enabling comprehensive tracking of HL setpoints. These algorithms employ a Tracking MPC that establishes an optimal energy program by tracking SOC, LOH, and HESS/MEG power setpoints provided by the HL.

CAT II algorithms have been effectively used in designing two-level MPC-based EMSs for power generation in residential microgrids [24]. Similar architectures have been proposed for managing microgrids with

cogeneration systems and gas generation, as described in [35] and [36], respectively. Additionally, [29] introduces a Tracking MPC for managing optimal load sharing in microgrids with HESS composed of several ESS with different dynamics. More advanced solutions are explored in [8,37], where robust and stochastic Tracking MPCs address uncertainties in microgrid generation and demand.

Although CAT II algorithms show improved performance over CAT I, they introduce additional complexities due to the multi-objective problem definition, which often necessitates weighting factors. Determining these factors is challenging, frequently relying on trial-and-error methods, which can compromise the economic optimality achieved by the HL. Furthermore, CAT II algorithms inherit some of the drawbacks of CAT I algorithms, such as increased solution multiplicity.

Finally, CAT III algorithms represent a hybrid MPC, combining Tracking MPC and Economic MPC principles. These algorithms incorporate tracking functions similar to those in CAT II while also including cost terms in the objective function. This integration ensures that tracking HESS and MEG references does not compromise the economic performance of the microgrid at each sampling period. Cost terms in CAT III algorithms penalize excessive use of the MEG and/or cyclic operation of the HESS, accounting for factors like HESS degradation costs and energy purchase/sale costs from the MEG.

Due to their intrinsic complexity, CAT III algorithms are relatively rare in the scientific literature for the microgrid architecture under study. A simple example of a CAT III algorithm was validated in [38] for the design of two-level MPC-based EMS for microgrid control with HESS. The weighted objective function of the LL controller considers SOC and LOH tracking while minimizing MEG costs to ensure consistent MEG usage. Finally, a more complex variant was developed in [16,39] for an EMS based on a four-level MPC. This design manages microgrids operating as electricity market agents, with the LL controller incorporating a weighted objective function that tracks SOC and LOH references while accounting for degradation costs (cycles and operational time) and operation and maintenance (O&M) costs for the HESS and MEG.

Despite the significant advantages over previous approaches, this method has several drawbacks. First, defining weights requires in-depth knowledge of the microgrid, and these weights have no physical meaning, making them impossible to extrapolate to a new microgrid. Second, the monitoring of the HL cannot be guaranteed, as different weights and terms in the cost index may offset each other, preventing the HL from following the references for certain devices. Third, the HL lacks information on how to provide/consume energy within each sampling period. Therefore, following the average energy reference in the LL may not be the most economically efficient strategy.

From the literature review it can be deduced that, regardless of the type of algorithm used, the Tracking MPC (or Hybrid MPC) controllers proposed for LL design in EMS based on two-level MPCs may not guarantee the optimality achieved by the HL. This may have a negative impact on the economic viability of this type of microgrids, by increasing operating costs, or reducing their potential economic return. The performance achieved by this type of solutions will depend on many factors, e.g., the microgrid architecture and its application, fluctuations in generation and demand profiles, or the sampling period, among others.

To address the gaps identified in the literature review, this paper presents an EMS formulation based on a computationally approachable two-level economic MPC. This approach determines the optimal energy program that guarantees the best economic return in each sampling period. For this purpose, the proposed solution makes use of two Economic MPCs at the HL and LL levels. These are designed with economic objective functions that account for the specific operational characteristics of the HESS and MEG. By incorporating terminal constraints, the method not only ensures the achievement of the HL setpoints at the end of the PH but also identifies the best path to achieve them within each sampling period.

Thus, the main contributions of the paper can be summarised as follows:

- Development of a general and computationally approachable two-level Economic MPC-based EMS that improves the performance of LL-tracking MPC-based EMSs by considering the overall microgrid cost defined by MEG costs, O&M costs, and degradation in equipment usage in each sampling period. The use of economic objective functions avoids the use of weighting factors, which simplifies their design and reduces multiplicity.
- Development of a LL Economic MPC algorithm that ensures, through constraints in the control problem, the correct tracking of the optimal energy state setpoint of the HESS provided by the HL.
- Finally, the applicability and performance of the proposed EMS was validated against EMS based on Tracking MPC two-levels developed in the scientific literature for a renewable microgrid architecture with full a HESS.

Finally, to highlight the novelty of this research, Table 1 summarises its main characteristics in comparison with the analysed literature.

The rest of the article is organized as follows: The microgrid model is described in Section 2. The general formulation of the economic two-level MPC controller is developed in Section 3. The results provided by the proposed controller are presented, compared against other controllers, and discussed in Section 4. Finally, the main conclusions are highlighted in Section 5.

Microgrid model

Microgrid architecture

The microgrid, including each of its components, can be modelled based on the energy flows exchanged with the bus [9]. These energy flows are classified as either manipulable energy flows (MEFs), which can be controlled, or non-manipulable energy flows (non-MEFs), which have limited or no controllability. Non-MEFs are further categorized into power demands on the microgrid (P_{nMEF-}, such as load power) and power supplies to the microgrid (P_{nMEF+}, such as power generated from renewable sources). MEFs, in contrast, are essential for maintaining energy balance on the bus and include the charging and discharging of energy storage systems (ESS) and the main electricity grid (MEG) in grid-tie architectures. Within this framework, any microgrid architecture can be described as a combination of MEFs (associated with ESS and MEG) and non-MEFs (associated with loads and renewable generation). This approach will form the basis for defining the microgrid model in the following sections.

Modelling

After defining the energy flows in a generic architecture, the next step is to model the microgrid for its application in control strategies. This subsection outlines the general microgrid model, which follows the methodology and steps presented in the reference flowchart from previous works [9]. For brevity, only the essential aspects of the methodology are discussed here. Since this work focuses on demonstrating the technical feasibility and comparing the performance of the proposed algorithm with traditional two-level solutions, the model does not account for disturbances or uncertainties. However, these factors could be incorporated into both the model and the controller design, depending on their nature.

To balance accuracy and computational efficiency, the proposed microgrid model employs a linear piecewise model approach. This model approximates the non-linear behaviour of the microgrid as a function of the power flow direction, the number of ESSs (n) and the DC bus connection topology. To achieve this, each ESS's charging power (P_{ch_j}) and discharging power (P_{dis_j}) is expressed as $P_j = P_{dis_j} - P_{ch_j}$.

Table 1
Summary of MPC-based EMS proposals solutions found in the literature compared to the authors' proposal.

Ref.	MPC-based EMS				
	EMS Architecture	**Low-level MPC definition**	**Low-level MPC Cost function terms**	**High-level references**	**Reference tracking and method**
[30]	Two-level MPC	Tracking MPC CAT I	SOC & LOH tracking error	SOC, LOH	Not guaranteed Linear tracking error
[17,22,27,28,31,32]	Two-level MPC	Tracking MPC CAT I	HESS/MEG Power tracking error	HESS/MEG power	Not guaranteed Quadratic tracking error
[33,34]	Two-level MPC	Tracking MPC CAT I	MEG Power and HESS operating cycles tracking error	MEG power and HESS operating cycles	Not guaranteed Quadratic tracking error
[25]	Two-level MPC	Tracking MPC CAT I	MEG Power and Load Shifting factor tracking error	MEG power and Load Shifting factor	Not guaranteed Quadratic tracking error
[8,24,29,35–37]	Two-level MPC	Weighted Tracking MPC CAT II	SOC & LOH and HESS/MEG tracking error	SOC, LOH and HESS/MEG power	Not guaranteed Weighted quadratic tracking error
[38]	Two-level MPC	CAT III Weighted Hybrid Tracking MPC and Economic MPC	SOC & LOH tracking error MEG cost	SOC, LOH and MEG power	Not guaranteed Weighted quadratic tracking error
[16,39]	Four levels MPC	CAT III Weighted Hybrid Tracking MPC and Economic MPC	SOC & LOH tracking error Degradation and O&M cost	SOC, LOH and MEG power	Not guaranteed Weighted quadratic tracking error
Authors's approach	Bilevel MPC	Economic MPC	O&M cost Degradation cost	SOC and LOH	Guaranteed Terminal constraint

Similarly, the power purchased (P_{grid_p}) and sold (P_{grid_s}) to the MEG are represented as $P_{grid} = P_{grid_p} - P_{grid_s}$.

Using this modelling approach, this section will outline the methodology for developing the overall microgrid model. This includes the modelling of the microgrid's energy storage systems (ESS), the DC bus voltage (V_{BUS}) when its control is necessary, and finally, the power balance of the bus, which dictates microgrid operation regardless of its connection to the MEG. Regardless of the nature of the ESS and the power flow direction, its behaviour can generally be defined by a first-order discrete integrator, according to (1).

$$SOC_j(k+1) = SOC_j(k) + r^j_{ch} \cdot P_{ch_j}(k) - r^j_{dis} \cdot P_{dis_j}(k) \tag{1}$$

where r^j_{ch} and r^j_{dis} are the charging and discharging ratios for each ESS_j, calculated from the energy balance considering the nominal capacity CN_j (in Wh), its operating efficiency (η^j_{ch} and η^j_{dis}), and the sample time (T_s) according to (2).

$$r^j_{ch} = \frac{\eta^j_{ch}}{CN_j} \cdot T_s ; r^j_{dis} = \frac{1}{\eta^j_{dis} \cdot CN_j} \cdot T_s \tag{2}$$

Finally, the bus DC voltage variable (V_{BUS}) is considered only in microgrid architectures where the DC bus is passively supported by the direct connection of a BSS, without power converters. In such architectures, voltage control is necessary because maintaining the DC bus voltage within the desired range depends on proper synchronization between generation and demand in the main bus [9,40]. As a result, this becomes a global control issue that must be managed within the EMS. In contrast, microgrids with an active configuration (using power converters) regulate the DC bus voltage locally through the associated ESS. Based on the above, in passive architectures, V_{BUS} will be added as a new state variable in the model. To do so, starting from the desired BSS model, the necessary processes will be implemented to obtain a linear model according to the general equation (3).

$$V_{BUS}(k+1) \approx K_{V_{BUS}} \bullet V_{BUS}(k) + K_{SOC} \cdot SOC_j(k) + K_{Pch} \cdot P_{ch_j}(k) - K_{Pdis} \cdot P_{dis_j}(k) + v_k \tag{3}$$

where $K_{V_{BUS}}$, K_{SOC}, K_{Pch} and K_{Pdis} are the battery coefficients of V_{BUS}, SOC_j, P_{ch_j} and P_{dis_j} respectively, and v_k is the independent term result of the linearization process.

Equation (3) implies that the DC bus voltage is inherently governed by the voltage of the BSS. When power is injected into or extracted from the DC bus, the charging or discharging of the ESS directly alters its terminal voltage, causing the DC bus voltage to increase or decrease accordingly.

Based on the above and considering that the ESSs are the ones that determine the dynamics of the microgrid, its general model can be formulated as state-space equations according to (4).

$$\begin{aligned} x(k+1) &= Ax(k) + Bu(k) + d \\ y(k) &= x(k) \end{aligned} \tag{4}$$

where the state variables $x(k)$ coincide with the SOC_j of each ESS_j ($[SOC_1 \cdots SOC_n]^T$. Also, in microgrid topologies where the DC bus is supported by the direct connection of ESS, V_{BUS} can be integrated in the state vector when its control is required. To do so, the ESS_j associated with this variable must be identified and matched in the model with the corresponding manipulable variable. Finally, the outputs will coincide with the states, $y(k) = x(k)$, and the manipulated variables ($u(k)$) will be the charge/discharge powers of each ESS_j ($[P_{ch_1} P_{dis_1} \cdots P_{ch_n} P_{dis_n}]^T$). Thus, for a microgrid architecture composed of n ESSs, and without loss of generality, with DC bus supported by ESS_1, the general microgrid state-space model is shown in (5). This approach ensures adaptability to any microgrid, regardless of the bus type or ESS configuration.

$$\overbrace{\begin{bmatrix} SOC_1(k+1) \\ \vdots \\ SOC_n(k+1) \\ V_{BUS}(k+1) \end{bmatrix}}^{x(k+1)}_{(n+1,1)} = \overbrace{\begin{bmatrix} 1 & \cdots & 0 & 0 \\ \vdots & \ddots & \vdots & \vdots \\ 0 & \cdots & 1 & 0 \\ K_{SOC} & 0 & \cdots & K_{V_{BUS}} \end{bmatrix}}^{A}_{(n+1,n+1)} \overbrace{\begin{bmatrix} SOC_1(k) \\ \vdots \\ SOC_n(k) \\ V_{BUS}(k) \end{bmatrix}}^{x(k)}_{(n+1,1)} + \overbrace{\begin{bmatrix} r^1_{ch} & -r^1_{dis} & \cdots & 0 & 0 \\ \vdots & \vdots & \ddots & \vdots & \vdots \\ 0 & 0 & \cdots & r^n_{ch} & -r^n_{dis} \\ K_{Pch} & -K_{Pdis} & 0 & \cdots & 0 \end{bmatrix}}^{B}_{(n+1,2n)} \overbrace{\begin{bmatrix} P_{ch_1}(k) \\ P_{dis_1}(k) \\ \vdots \\ P_{ch_n}(k) \\ P_{dis_n}(k) \end{bmatrix}}^{u(k)}_{(2n,1)} + \overbrace{\begin{bmatrix} 0 \\ \vdots \\ 0 \\ v_k \end{bmatrix}}^{d}_{(n+1,1)} \tag{5}$$

The microgrid must maintain power balance according to equation (6) [9], considering energy conversion and transport losses, as well as auxiliary consumption ($Loss$). In isolated configurations, P_{grid} term is

zero. According to the established criterion, the powers associated with MEFs (P_{grid_p},P_{grid_s},P_{ch_j} and $P_{dis_j}\forall ESS_j$) and non-MEFs (P_{nMEF+}, P_{nMEF-}) are individually positive. However, for the power balance defined in equation (6), the injected and extracted power from the microgrid must have opposite signs. Therefore, powers injected into the DC bus (P_{grid_p},P_{dis_j} and P_{nMEF+}) are added as positive. In contrast, powers extracted from the DC bus (P_{grid_s},P_{ch_j} and P_{nMEF-}) are added as negative in the power balance equation (6). For the MEFs power (P_j and P_{grid}), the sign is determined by the previously defined power expressions ($P_{grid}=P_{grid_p}-P_{grid_s}$ and $P_j=P_{dis_j}-P_{ch_j}$) following the same criteria.

$$P_{nMEF+}-P_{nMEF-}-Loss(k)+P_{grid}(k)+\sum_{j=1}^{n}P_j(k)=0 \tag{6}$$

In this context, $Loss(k)$ term encompasses all total losses in the microgrid that have not been previously accounted for, as described in equation (7). These losses do not include those related to non-MEFs, as the net energy flows to and from the bus (P_{nMEF+} and P_{nMEF-}) already account for these losses in the respective terms.

$$Loss(k)=\sum_{i=MEF}^{|MEF|}Loss_i(k)\cdot P_i(k)+Loss_i^{BoP}\cdot WT_i \tag{7}$$

Where $Loss_i^{BoP}$ and $Loss_i$ are the balance of plant (BoP) and the variable losses of MEF_i, respectively, while WT_i is a binary variable defining whether the MEF_i is operating. $WT_i=1$ if the MEF_i injects ($i=\{dis_1,\cdots,dis_n,grid_p\}$) or extracts ($i=\{ch_1,\cdots,ch_n,grid_s\}$) energy, *i.e.* if it operates; and $WT_i=0$ if the MEF_i does not operate. According to equation (7), $Loss(k)$ term consists of two types of losses: variable and fixed. The first term models the variable power losses as a function of the power P_i, while the second term represents the fixed losses, labelled $Loss_i^{BoP}$.

Two-level hierarchical MPC-based EMS control of microgrid

As mentioned above, this work compares two computationally accessible two-level MPC based-EMSs approaches, both aimed at minimizing the operating cost of the microgrid, while considering fundamental technical aspects in its operation. Each approach defines an MPC controller for the resolution of each of its two levels. As mentioned earlier, this study aims to demonstrate the technical viability of the proposed algorithm and compare its performance with traditional two-level solutions. Therefore, uncertainties in generation and demand forecasts, along with controller design parameters (such as costs), are not considered.

According to the two-level philosophy, each strategy is composed of an HL and an LL (see Fig. 2). Generally, the HL develops a long-term economic optimisation and has a longer sampling period Ts_{HL} with a long-term horizon PH_{HL}. For this purpose, this level predicts average energy consumption and production over the sampling periods, determining the total energy to be provided or consumed by each device in the microgrid. However, it does not specify how to allocate this energy within each sampling period (the same always, more at the beginning than at the end, more at the end than at the beginning, etc). To address this limitation, the LL operates with a shorter sampling period Ts_{LL} and a short-term horizon PH_{LL}. Its role is to use the information provided by the HL (which has long-term forecasting) and manage how the energy is provided or consumed within each sampling period. The strategy applied in the design of the LL largely influences the economic response of the microgrid.

The first strategy evaluated is the one most widely used in the literature. It features a HL that focuses on long-term economic optimisation, while the LL tracks the average power and/or SOC references (P_i^{ref} and SOC_j^{ref}) provided by the HL for each sampling period. This strategy will be referred to as "tracking approach" in this paper.

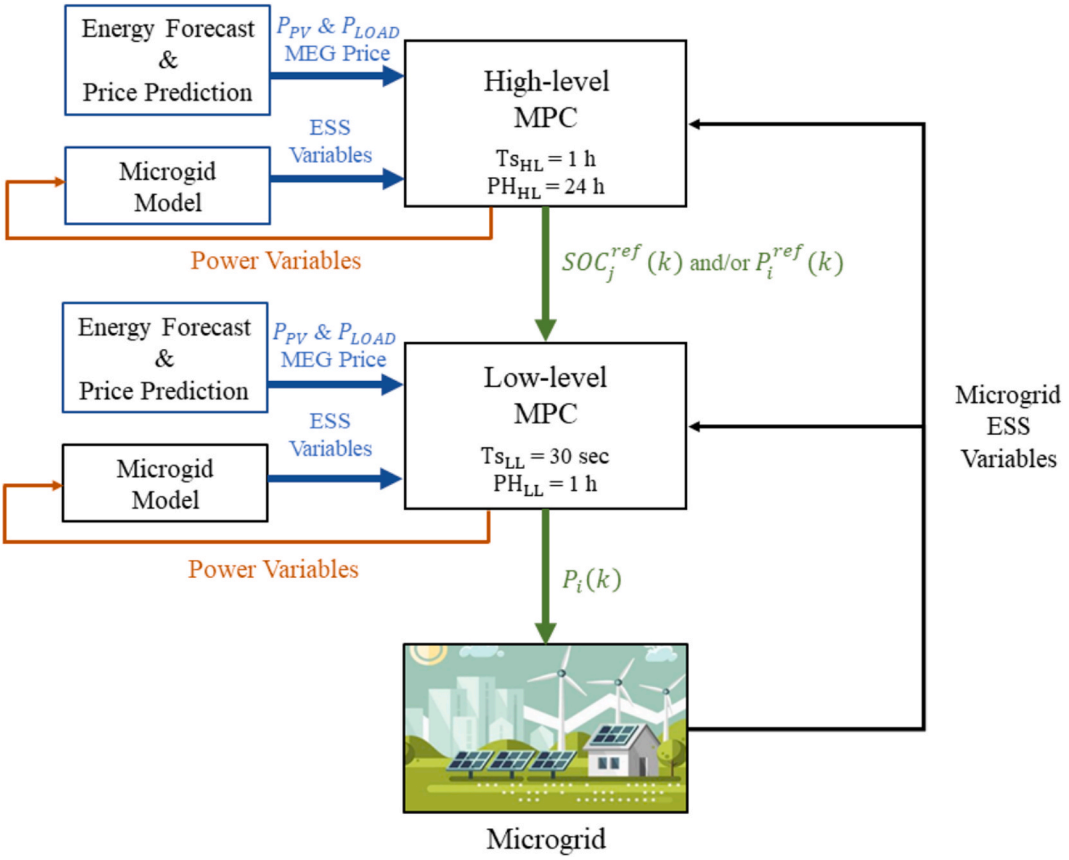

Fig. 2. Two-level hierarchical MPC controller architecture.

The second strategy is based on the new approach presented in this article. Like the previous one, it has a HL focused on long-term economic optimisation. However, its LL also performs economic optimisation, using the SOC reference (SOC_j^{ref}) of each ESS, obtained from the HL, to determine the target SOC to be reached at the end of PH_{LL}. This strategy will be referred to as "economic approach" in this paper.

Since both strategies require an economic HL, it is reasonable to use the same HL for a fair comparison between the two bilevel MPCs. The main difference will lie in the design of the LL: the first strategy uses a tracking approach (as found in the literature), while the second uses the economic approach (proposed in this paper).

The fundamentals of the HL and the two LLs to be evaluated will be presented below.

High level

The HL is responsible for determining the best strategy from an economic perspective respecting fundamental technical aspects in its operation. For this, it relies on long-term energy forecast, which include both renewable energy production and demand. In a microgrid, particularly with solar panels, daily cyclical behaviour is common. For instance, during the day, excess energy can be produced due to sunlight, but in the afternoon or evening, when the sun sets, there may be an energy deficit. Similarly, consumption patterns often follow daily trends (lower consumption in the morning when no one is home, and higher consumption in the evening when people return). Therefore, it makes sense to define a prediction horizon (PH_{HL}) of 24 h to optimise the full daily cycle.

To ensure the MPC is computationally feasible in real-time applications, it must have an adequate sampling period (Ts_{HL}). A very short sampling period would significantly increase computational cost. For its correct choice, sampling period should also consider specific application considerations. For example, in some countries, the price for buying and selling energy to the grid is set on an hourly basis. To align with this discretization (as done in this work), using a Ts_{HL} longer than 1 h would be impractical, as it would miss the opportunity to account for hourly price changes. Finally, it is important to consider the relationship between Ts_{HL} and PH_{LL} (which are usually set to be equal), as the powers, and/or the level of energy stored in the ESS after a Ts_{HL} will serve as the reference for the LL.

In the literature, each author uses a different cost minimization index (economic, weighted, etc.). To compare the two approaches evaluated in this work (tracking and the proposed strategy), the generic economic index introduced in [9] and shown in (8) is used. This index associates all terms with an economic cost (in this case in €) [9]. This ensures that all the summands have the same units, making is more intuitive for the designer. Despite this, the index carries out a technical–economic optimization for microgrid management, with cost terms specifically designed to minimize operation and maintenance costs, while also accounting for technical aspects of the microgrid's operation from an economic perspective.

In addition, this index is general, parameterizable, simple, easily interpretable, and reproducible in different microgrid architectures. This generality is achieved by defining an objective function that incorporates various cost terms, fixed, variable, start-up, and degradation-related, which can be selectively included or omitted based on the specific requirements of the application. This index is calculated for each time step k of the PH_{HL} and for each MEF_i of the microgrid.

$$J=\sum_{k=1}^{PH_{HL}}\left(\sum_{i=MEF}^{|MEF|}C_i^{var}\cdot P_i(k)+C_i^{fix}\cdot WT_i(k)+C_i^{start}\cdot Start_i(k)+C_i^{degr}\cdot\delta P_i^2(k)\right) \tag{8}$$

According to (8), the term $C_i^{var}\cdot P_i(k)$ determines the variable costs of each MEF_i when operating at a power (P_i). The term $C_i^{fix}\cdot WT_i(k)$ accounts for the fixed costs associated with the operation of each MEF_i, where the binary variable WT_i indicates whether MEF_i is operating. Therefore, the first two terms are intended to reduce the microgrid's operation and maintenance costs. On the other hand, the next two terms incorporate technical aspects into the optimization by encouraging a more cautious use of equipment that requires it, penalizing unnecessary startups or sudden changes in operating power, such as those of HBSS. Specifically, the term $C_i^{start}\cdot Start_i(k)$ determines the startup costs of each MEF_i, whit the binary variable $Start_i$ indicating whether the device i is switched on at the time instant k. Specifically, $Start_i(k)=WT_i(k)\bigwedge WT_i(k-1)$.

In a microgrid there may be devices whose repetitive switching on and off can considerably reduce their lifetime (e.g. fuel cell and electrolyser) [1,41]. To mitigate this issue, the switching on and off of these devices can be penalized. Lastly, the term $C_i^{degr}\cdot\delta P_i^2(k)$ determines the degradation costs associated with fluctuations in the operating power of each MEF_i. Frequent changes in energy demand or production in a microgrid can be undesirable, so this term penalizes such fluctuations. However, these fluctuations should not be penalized during the startup and shut-down processes [42]. Therefore, δP_i represents the power variation as a function of the binary variable Y_i, which indicates when a MEF_i has completed its startup and shut-down process. This considers the necessary sampling periods to reach nominal power or to fully stop the device (NTs_i), as defined in equation (9).

$$\delta P_i=\Delta P_i\cdot Y_i$$

where:

$$Y_i=(WT_i(k)\wedge WT_i(k-1)\wedge\cdots\wedge WT_i(k-NTs_i)) \tag{9}$$

Low level

Low level tracking approach

The LL tracking approach is responsible for implementing the strategy that guarantees the optimal tracking of the average references obtained by the HL at each sampling period. Typically, the LL prediction horizon (PH_{LL}) matches the sample period of the HL ($PH_{LL}=Ts_{HL}$). In this work, the commonly used generic cost index, as shown in equation (10), will be employed [17,22,27,31]. Some authors exclude certain terms, but this can be achieved by using null weights on those terms:

$$J=\sum_{k=1}^{PH_{LL}}\left(\sum_{i=MEF}^{|MEF|}\omega_{P_i}\left(P_i(k)-P_i^{ref}\right)^2+\omega_{Start_i}\cdot Start_i(k)+\omega_{\delta P_i}\cdot\delta P_i{}^2(k)\right)+\sum_{j=1}^{n}\left(\omega_{SOC_j}\left(SOC_j(k)-SOC_j^{ref}\right)^2\right) \tag{10}$$

This index uses the information for each time step k of the PH_{LL}, as well as for each ESS of the microgrid (with n representing the number of ESS) and each MEF_i ($ch_1, dis_1, \cdots, ch_n, dis_n, grid_p, grid_s$). The index to be optimised includes several terms, each weighted by specific factors to be defined (ω_{P_i}, ω_{Start_i}, $\omega_{\delta P_i}$ y ω_{SOC_j}).

According to (10), the term $\omega_{P_i}\left(P_i(k)-P_i^{ref}\right)^2$ seeks to follow the power reference provided by the HL for each MEF_i. Since tracking the reference is not enough on its own, and the method of tracking is important, it is essential to promote conservative use of the certain ESSs. To this end, analogous to the HL economic index, the second term, $\omega_{Start_i}\cdot Start_i(k)$, penalises frequent startup and shut-down cycles of devices that generate/consume power in each MEF_i. The term $\omega_{\delta P_i}\cdot\delta P_i{}^2(k)$ penalises power fluctuations. Both $Start_i$ and δP_i are defined similarly to their counterparts in the HL economic index.

Finally, the term $\omega_{SOC_j}\left(SOC_j(k)-SOC_j^{ref}\right)^2$ referring to ESS storage levels. This term aims to ensure that the ESS storage level follow the reference values provided by the HL.

Based on the generic architecture of a hierarchical two-level MPC

shown in Fig. 1, along with the design considerations for the HL, the LL tracking approach, and the unidirectional information flow from the HL to the LL, the architecture of the hierarchical two-level tracking MPC controller is shown in Fig. 2.

Low level economic approach

As previously discussed, the objective of this LL is to reach the optimal ESS level references. However, there are many possible strategies that can reach the optimal ESS level at the end of the PH_{LL}, and the method to achieve this will affect the operating cost of the microgrid, potentially undermining the results obtained from the HL. To ensure the most economical solution, the LL is again defined based on an economic optimisation (LL economic). This approach allows the MPC to determine the economically optimal strategy in the short-term, subject to reaching the optimal level of ESS (obtained by the HL with the long-term prediction) at the end of the PH_{LL} (by means of the final constraints $SOC_j(PH_{LL}) = SOC_j^{ref}$). For this purpose, this MPC uses the same generic economic index defined in the HL for a PH_{LL} (see equation (8)).

Again, based on the generic architecture of a hierarchical two-level MPC shown in Fig. 1, along with the design considerations for the HL, the LL economic approach, and the unidirectional information flow from the HL to the LL, the architecture of the hierarchical two-level economic MPC controller is shown in Fig. 2.

Since the economic LL approach is derived from the same objective function as the HL, the proposed two-level economic MPC control is inherently general and adaptable to any microgrid architecture. This adaptability stems from the flexibility of the control problem defined by the objective function in (8).

Optimisation problem

Based on the above, the MPC-based EMS for each level and each approach is defined as the optimisation problem defined in equation (11). In this problem, the decision variables $z = [P_i(k),\ WT_i(k), Start_i(k), \delta P_i(k)]$ are defined for each MEF_i of the microgrid.

$$\min J$$

Subject to:

$$\underline{P_i} \cdot WT_i(k) \le P_i(k) \le \overline{P_i} \cdot WT_i(k) \forall i \in MEF_i$$

$$\underline{\Delta P_i} \le \Delta P_i(k) \le \overline{\Delta P_i} \forall i \in MEF_i$$

$$WT_{ch_j}(k) + WT_{dis_j}(k) \le 1 \ \forall j \in ESS_j$$

$$WT_{grid_s}(k) + WT_{grid_p}(k) \le 1$$

$$\underline{x_l} \le x_l(k) \le \overline{x_l} \ \forall x_l(k)$$

$$P_{nMEF+} - P_{nMEF-} - Loss(k) + P_{grid}(k) + \sum_{j=1}^{n} P_j(k) = 0 \quad (11)$$

where J is the generic economic cost index defined in (8), for all levels and MPCs used in this work, except for the LL tracking approach, where the index is defined in (10).

Case studies: results & discussion

This section validates the proposed two-level hierarchical economic MPC-based EMS using the methodology defined in [9]. This methodology allows defining the microgrid model, as well as the MPC controller for each level. For its validation, the proposed EMS was designed for a microgrid architecture under study, and the results obtained were compared with the widely used two-level hierarchical tracking MPC-based EMS approach from the literature, which incorporates the two classical tracking functions. Various simulations were conducted in MATLAB Simulink® using the YALMIP toolbox and the IBM CPLEX Optimiser solver for MIQP optimisation problems.

Case study

Microgrid architecture

As discussed in the previous section, this study aims to develop an EMS based on a two-level MPC architecture, designed to optimise the energy management of renewable microgrids with HESS. Moreover, the response of the EMS-microgrid set should increase the performance in technical and economic terms compared to existing solutions in the scientific literature.

To ensure a fair comparison between different EMS proposals, the design, implementation, and validation should be based on a well-established and general microgrid architecture. However, the proposed architecture and control laws can be adapted to any microgrid type by following the modelling and controller design methodology outlined in Sections 2 and 3.

Various microgrid architectures have been presented and analysed in the scientific literature, being perhaps the most studied the grid-tie residential DC microgrid architecture with a HESS, using BSS and HBSS [38,43,44]. For this reason, this type of microgrid architecture has been chosen for this study. The microgrid architecture under study is shown in Fig. 3.

In this architecture, four key systems are integrated onto a DC bus: generation, demand, ESS, and MEG. The renewable generation is provided by a photovoltaic field ($P_{nMEF+} = P_{PV}$), which is connected to the DC bus via a power converter. The renewable generation profile is based on typical radiation data for the city of Huelva, Spain (37°15′59″ N 6°56.402′ O).

On the other hand, the demand of the microgrid is determined by the sum of three power consumption profiles: household appliances and lighting (P_{HA}), heating, ventilation, and air conditioning system (P_{HVAC}), and the vehicle charging demand (P_{EV}). Similarly, each demand is connected to the DC bus through its appropriate power converter. The sum of the above demands determines the load power of the microgrid ($P_{nMEF-} = P_{HVAC} + P_{HA} + P_{EV}$). The consumption profiles correspond to a typical residential application profile provided by the Spanish Institute for Energy Diversification and Saving.

For simplicity and to align with the main objective of the research, this study does not consider uncertainties in the renewable generation and demand profiles in the validation and comparative economic analysis with traditional hierarchical two-level EMS.

The ESS is a hybrid system (HESS) that combines two technologies with different roles and response times, operating in parallel to provide better dynamic response and long-term storage capacity. Specifically, it consists of a BSS for short-to medium-term ESS (P_{bat}), which is directly connected to the DC bus. The BSS absorbs power mismatches between energy generation and demand and helps control the DC bus voltage, without the need to implement additional control laws, even during abrupt changes in power generation or demand. In contrast, this topology requires the EMS to control the charging and discharging of the BSS to maintain the desired bus voltage range. In this case, the BSS is modelled using a first-order Thevenin equivalent model, which also governs the DC bus voltage [45].

The second component of the ESS is an HBSS designed for long-term ESS. This system covers the complete cycle of hydrogen use, including production, storage, and subsequent generation of electrical energy. For this purpose, the HBSS consists of an electrolyser ($P_{ch_{H2}}$), a hydrogen storage tank, and a fuel cell stack ($P_{dis_{H2}}$). Each unit of the HBSS is integrated into the DC bus via its own power converter.

Finally, the microgrid also includes a bidirectional connection to the MEG, via appropriate power converters, allowing for power balance in cases of energy surplus or deficit. This connection also enables the microgrid to engage in economic transactions by buying and selling

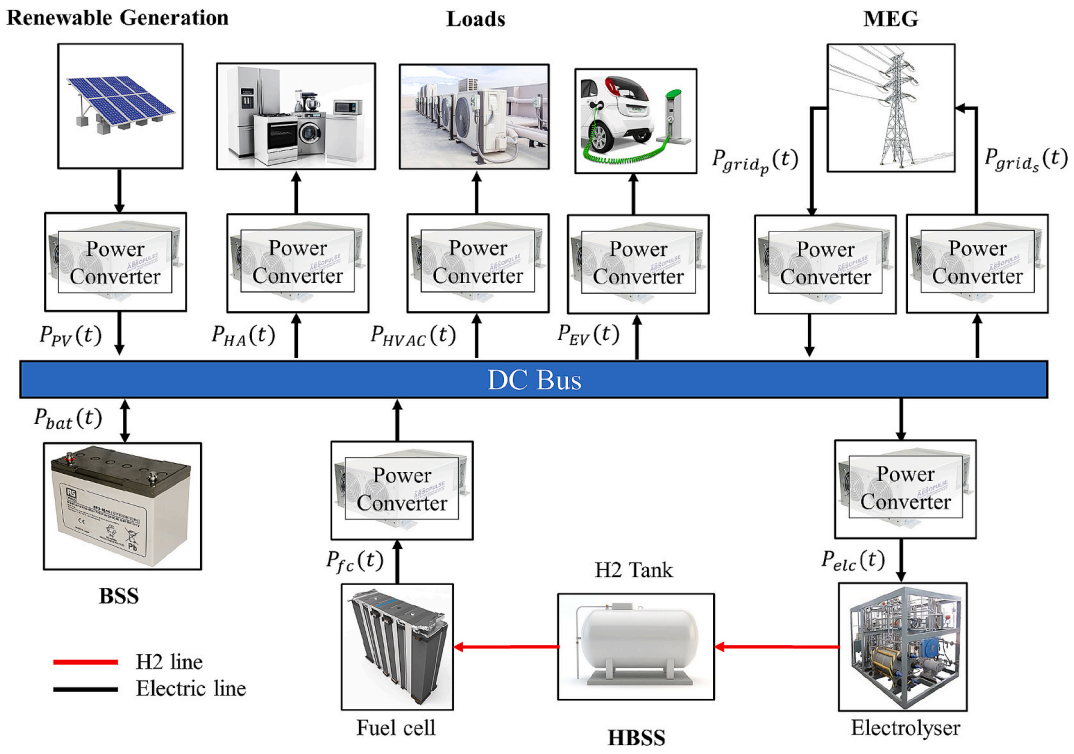

Fig. 3. Proposed microgrid architecture.

energy from the MEG.

Sizing the microgrid is a complex task, as it depends on various factors such as the availability of renewable resources, consumption profiles, and equipment costs. Since sizing is not the objective of this work, the general parameters of the equipment that make up the microgrid have been defined based on the experimental microgrid that the authors have at their disposal at CITES. More detailed information about the microgrid can be found in [41]. Following the methodology described in [9] and the general state-space model of a microgrid presented in (5), the specific model of the microgrid under study, along with its key parameters, is outlined in Tables 2 and 3.

MPC-based EMS

For the definition of the MPC, it is necessary to establish the constraints, losses, and cost terms of each MEF (or weight in the MPC tracking approach), which determine the microgrid architecture according to the proposed methodology in [9]. The constraints arise from the physical limits of the devices, the manufacturer's recommendations, state variables, and definition of decision variables such as $Start_i$ ($Start_i(k) = WT_i(k) \wedge \overline{WT_i(k-1)}$) and $\delta P_i(\delta P_i(k) = \Delta P_i(k) \wedge Y_i(k)$, with $Y_i(k) = WT_i(k) \wedge \overline{WT_i(k-1)}$). These constraints are formulated by converting logical relations into mixed-integer inequalities [46,47]. In addition, the LL economic approach has additional constraints to guarantee the ESS reaches the levels when $t = PH_{LL}$ ($SOC_{bat}(PH_{LL}) = SOC_{bat}^{ref}$, $SOC_{H2}(PH_{LL}) = SOC_{H2}^{ref}$). In this example, and based on the HL and LL design considerations described in section 3, a HL with a $PH_{HL} = 24$h and $Ts_{HL} = 1$h is used, while the LL has a $PH_{LL} = 1$h and $Ts_{LL} = 30$sec.

The costs used in the MPCs are listed in Table 3, excluding the weights of the LL tracking approach, which are defined later. Only variable O&M costs are considered for the BSS, with no losses due to its direct connection to the DC bus. For the HBSS, fixed operation, maintenance, and startup costs are included, but variable costs are excluded since the device consumption is part of the energy balance ($Loss_i^{BoP}$). Degradation costs for the LL are included, but these must be lower than startup costs to prevent switching the device on and off from being more cost-effective than to vary its power. Then, the degradation cost is defined as $C_i^{degr} = \frac{C_i^{start}}{\overline{\Delta P_i}^2}$ (where $\overline{\Delta P_i}$ is the maximum value of δP_i). Variable losses due to power converters and BoP are also considered. For the MEG, variable energy purchase costs (see Table 4) and fixed energy sale costs are considered, but there are no fixed startup or degradation costs. The connection to the DC bus involves variable losses from the power converters.

Table 5 defines the weights relative to the index used in the LL tracking approach (see equation (10)). To evaluate the performance of the proposed economic EMS with respect to different indices from the scientific literature and to highlight the importance and impact of weight tuning, three controller settings with different weight calculation techniques are defined.

For the first controller setting, null weights ω_{Start_i}, $\omega_{\delta P_i}$ and ω_{SOC_j} are defined, which results in a classical power tracking problem. In this way, only the weights ω_{P_i} exist for each MEF_i. These weights are set to 1 (unitary), meaning all discrepancies in powers are treated equally, avoiding any complexity in defining the weights.

The second controller setting aims for better microgrid performance by fully defining the index. The large number of parameters is handled by treating the index terms with similar priority. The weights penalizing power discrepancies are defined as for the first controller setting, and additional weights are introduced to penalize: (1) differences in the SOC of the ESS (ω_{SOC_j}), (2) startups of the hydrogen systems (ω_{Start_i}), and (3) fluctuations in the power of the hydrogen systems ($\omega_{\delta P_i}$). These weights are normalized based on the maximum power of each device, and the ones penalizing power fluctuations are normalized with respect to the maximum expected value.

For the third controller setting, the weights are chosen consciously according to the desired role of the ESSs and the grid in the microgrid. First, the BSS is expected to act as a short-term ESS, absorbing/providing the instantaneous power peaks, while the HBSS will absorb/provide energy as a long-term ESS. Finally, the grid must ultimately ensure the power balance according to (6). Therefore, weights are defined: $\omega_{P_{ch/dis\_bat}} < \omega_{P_{ch/dis_{H2}}} < \omega_{P_{grid_{s/p}}}$. Specific values are defined by trial and

Table 2
Necessary parameters for the definition of the micro-grid model and HL and LLs MPC controllers.

Controller	Model
HL	$\begin{bmatrix} SOC_{bat}(k+1) \\ SOC_{H2}(k+1) \end{bmatrix} = \begin{bmatrix} 1 & 0 \\ 0 & 1 \end{bmatrix} \begin{bmatrix} SOC_{bat}(k) \\ SOC_{H2}(k) \end{bmatrix} + \begin{bmatrix} r_{ch}^{bat} & -r_{dis}^{bat} & 0 & 0 \\ 0 & 0 & r_{ch}^{H2} & -r_{dis}^{H2} \end{bmatrix} \begin{bmatrix} P_{ch_{bat}}(k) \\ P_{dis_{bat}}(k) \\ P_{ch_{H2}}(k) \\ P_{dis_{H2}}(k) \end{bmatrix}$
LL	$\begin{bmatrix} SOC_{bat}(k+1) \\ SOC_{H2}(k+1) \\ V_{BUS}(k+1) \end{bmatrix} = \begin{bmatrix} 1 & 0 & 0 \\ 0 & 1 & 0 \\ K_{SOC} & 0 & K_{V_{BUS}} \end{bmatrix} \begin{bmatrix} SOC_{bat}(k) \\ SOC_{H2}(k) \\ V_{BUS}(k) \end{bmatrix} + \begin{bmatrix} r_{ch}^{bat} & -r_{dis}^{bat} & 0 & 0 \\ 0 & 0 & r_{ch}^{H2} & -r_{dis}^{H2} \\ K_{Pch} & K_{Pdis} & 0 & 0 \end{bmatrix} \begin{bmatrix} P_{ch_{bat}}(k) \\ P_{dis_{bat}}(k) \\ P_{ch_{H2}}(k) \\ P_{dis_{H2}}(k) \end{bmatrix} + \begin{bmatrix} 0 \\ 0 \\ 0 \\ v_k \end{bmatrix}$
	Cost function
HL	$J = \sum_{k=1}^{PH} \sum_{i=MEF}^{\lvert MEF \rvert} C_i^{var} \cdot P_i(k) \cdot T_s + C_i^{fix} \cdot WT_i(k) \cdot T_s + C_i^{start} \cdot Start_i(k)$
LL economic	$J = \sum_{k=1}^{PH} \sum_{i=MEF}^{\lvert MEF \rvert} C_i^{var} \cdot P_i(k) \cdot T_s + C_i^{fix} \cdot WT_i(k) \cdot T_s + C_i^{start} \cdot Start_i(k) + C_i^{degr} \cdot \delta P_i^2(k)$
LL tracking	$J = \sum_{k=1}^{\mathrm{PH}} \left(\sum_{i=\mathrm{MEF}}^{\lvert \mathrm{MEF} \rvert} \omega_{P_i} \left(\mathrm{P_i(k)} - \mathrm{P_i^{ref}} \right)^2 + \omega_{Start_i} \cdot \mathrm{Start_i(k)} + \omega_{\delta P_i} \cdot \delta \mathrm{P_i}^2(\mathrm{k}) \right) + \sum_{j=1}^{n} \left(\omega_{SOC_j} \left(\mathrm{SOC_j(k)} - \mathrm{SOC_j^{ref}} \right)^2 \right)$
	Decision variables
All MPCs	$P_{ch_{bat}}(k), P_{dis_{bat}}(k), P_{ch_{H2}}(k), P_{dis_{H2}}(k), P_{grid_s}(k), P_{grid_p}(k), WT_{ch_{bat}}(k), WT_{ch_{H2}}(k), WT_{dis_{H2}}(k), WT_{grid_p}(k), Start_{ch_{H2}}(k)^*, Start_{dis_{H2}}(k)^*$
LL economic	$\delta P_{ch_{H2}}(k), \delta P_{dis_{H2}}(k)$
	Constraints
All MPCs	$\underline{P_{ch_{bat}}} \cdot WT_{ch_{bat}}(k) \le P_{ch_{bat}}(k) \le \overline{P_{ch_{bat}}} \cdot WT_{ch_{bat}}(k) \underline{P_{dis_{bat}}} \cdot \left(1 - WT_{ch_{bat}}(k)\right) \le P_{dis_{bat}}(k) \le \overline{P_{dis_{bat}}} \cdot \left(1 - WT_{ch_{bat}}(k)\right) \underline{P_{ch_{H2}}} \cdot WT_{ch_{H2}}(k) \le P_{ch_{H2}}(k) \le \overline{P_{ch_{H2}}} \cdot WT_{ch_{H2}}(k) \underline{P_{dis_{H2}}} \cdot WT_{dis_{H2}}(k) \le P_{dis_{H2}}(k) \le \overline{P_{dis_{H2}}} \cdot WT_{dis_{H2}}(k) \underline{P_{grid_p}} \cdot WT_{grid_p}$
	$(k) \le P_{grid_p}(k) \le \overline{P_{grid_p}} \cdot WT_{grid_p}(k) \underline{P_{grid_s}} \cdot \left(1 - WT_{grid_p}(k)\right) \le P_{grid_s}(k) \le \overline{P_{grid_s}} \cdot \left(1 - WT_{grid_p}(k)\right) \underline{SOC_{bat}} \le SOC_{bat}(k) \le \overline{SOC_{bat}}; \underline{SOC_{H2}} \le SOC_{H2}(k) \le \overline{SOC_{H2}} \underline{\Delta P_{els}} \le \Delta P_{els}(k) \le \overline{\Delta P_{els}}; \underline{\Delta P_{fc}} \le \Delta P_{fc}(k) \le \overline{\Delta P_{fc}} Start_i(k) = WT_i$
	$(k) \wedge \ WT_i(k-1)^* P_{dis_{bat}}(k)\left(1 + Loss_{dis_{bat}}\right) - P_{ch_{bat}}(k)\left(1 + Loss_{ch_{bat}}\right) + P_{dis_{H2}}(k)\left(1 + Loss_{dis_{H2}}\right) + WT_{dis_{H2}}(k) \cdot Loss_{dis_{H2}}^{BoP} - P_{ch_{H2}}(k)\left(1 + Loss_{ch_{H2}}\right) + WT_{ch_{H2}}(k) \cdot Loss_{ch_{H2}}^{BoP} + P_{grid_s}(k)\left(1 + Loss_{grid_s}\right) - P_{grid_p}(k)\left(1 + Loss_{grid_p}\right) + P_{nMEF+}(k) - P_{nMEF-}(k) = 0$
LL	$\underline{V_{BUS}} \le V_{BUS}(k) \le \overline{V_{BUS}}$
HL	$SOC_{bat}(0) = SOC_{bat}(PH_{HL}), SOC_{H2}(0) = SOC_{H2}(PH_{HL})$
LL economic	$\delta P_i(k) = \Delta P_i(k) \wedge Y_i(k)$, with $Y_i(k) = WT_i(k) \wedge WT_i(k-1)$
	$SOC_{bat}(PH_{LL}) = SOC_{bat}^{ref}, SOC_{H2}(PH_{LL}) = SOC_{H2}^{ref}$

* *Not considered for LL tracking approach.*

Table 3
Design parameters, costs, constraints and losses defined.

ESS parameters								
$CN_{bat} = 28.8$ kWh	$\eta_{ch}^{bat} = 0.934$		$\eta_{dis}^{bat} = 1$	$CN_{H2} = 24$kWh		$\eta_{ch}^{H2} = 0.7$	$\eta_{dis}^{H2} = 0.5$	
$K_{V_{BUS}} = 0.01$	$K_{SOC} = 30$			$K_{Pch} = 0.002$		$K_{Pdis} = 0.002$	$v_k = 355$	
MPC Parameters & Constraints								
MEF_i	C_i^{var}	C_i^{fix}	C_i^{start}	C_i^{degr}	$[\underline{P_i}, \overline{P_i}]$	$[\underline{\Delta P_i}, \overline{\Delta P_i}]$	$Loss_i$	$Loss_i^{BoP}$
ch_{bat}	$0.4€/MWh$	–	–	–	$[0, 10]kW$	[-10, 10]kW	–	–
dis_{bat}	$0.4€/MWh$	–	–	–	$[0, 6]kW$	[-6, 6]kW	–	–
ch_{H2}	–	0.005€/h	0.05€	3.1e-9€/W^{2*}	[1,5]kW	[-5, 5]kW	0.025	800W
dis_{H2}	–	0.01€/h	0.05€	8e-9€/W^{2*}	[1, 3.5]kW	[-3.5, 3.5] kW	0.025	300W
$grid_p$	Table 4	–	–	–	[0, 6]kW	[-6, 6] kW	0.05	–
$grid_s$	$60€/MWh$	–	–	–	[0, 10]kW	[-10, 10]kW	0.05	–
State Vector Constraints								
$\overline{SOC_{bat}} = 90$ %, $\underline{SOC_{bat}} = 55$ %, $\overline{SOC_{H2}} = 100$ %, $\underline{SOC_{H2}} = 10$ %, $\overline{V_{BUS}} = 450$ V, $\underline{V_{BUS}} = 330$V								
Initial conditions								
$V_{BUS}(0) = 375V$, $SOC_{bat}(0) = 55$ %, $SOC_{H2}(0) = 10$ %								

* *For the HL of both approaches this cost is not considered ($C_{ch/dis_{H2}}^{degr} = 0$).*

Table 4
MEG hourly power purchase price on 08/23/2023 in Spain.

Time	Price (€/***MWh***)	Time	Price (€/***MWh***)	Time	Price (€/***MWh***)	Time	Price (€/***MWh***)
08–09 h	221.63	14–15 h	171.12	20–21 h	282.51	02–03 h	155.51
09–10 h	196.62	15–16 h	171.74	21–22 h	296.13	03–04 h	149.13
10–11 h	223.31	16–17 h	177.15	22–23 h	238.85	04–05 h	145.63
11–12 h	217.61	17–18 h	196.46	23–00 h	208.51	05–06 h	149.34
12–13 h	216.55	18–19 h	246.94	00–01 h	183.67	06–07 h	176.24
13–14 h	216.19	19–20 h	264.82	01–02 h	178.46	07–08 h	193.68

Table 5
Weight defined for the cost index of the LL tracking approach.

Controller Setting	$\omega_{P_{ch/dis\_bat}}$	$\omega_{P_{ch/dis_{H2}}}$	$\omega_{P_{grid_{p/s}}}$	$\omega_{Start_{ch/dis_{H2}}}$	$\omega_{\delta P_{els/fc}}$	$\omega_{SOC_{bat}}$	$\omega_{SOC_{H2}}$
1	$\frac{1}{\overline{P_{ch/dis_{bat}}}^2}$	$\frac{1}{\overline{P_{ch/dis_{H2}}}^2}$	$\frac{1}{\overline{P_{grid_{p/s}}}^2}$	0	0	0	0
2	$\frac{1}{\overline{P_{ch/dis_{bat}}}^2}$	$\frac{1}{\overline{P_{ch/dis_{H2}}}^2}$	$\frac{1}{\overline{P_{grid_{p/s}}}^2}$	1	$\frac{1}{\overline{\Delta P_{els/fc}}^2}$	1	1
3	$\frac{1}{\overline{P_{ch/dis_{bat}}}^2}$	$\frac{10^2}{\overline{P_{ch/dis_{H2}}}^2}$	$\frac{10^4}{\overline{P_{grid_{p/s}}}^2}$	10^3	$\frac{10^3}{\overline{\Delta P_{els/fc}}^2}$	1	1

error.

In the final formulation of the optimisation problem, as referenced in [9], a mixed integer quadratic programming (MIQP) approach is employed with a quadratic cost function, which will be solved at each level of the method. Based on the designed methodology, the decision variables, cost function, and constraints for the optimisation problem are detailed in Tables 2 and 3. The justification for the parameter values included in Table 3 is provided below.

Regarding the ESS design parameters, the nominal capacities are determined by the physical limits of the equipment. For efficiency calculations, a charging efficiency of 93.4 % (η_{ch}^{bat}) and a discharging efficiency (η_{dis}^{bat}) of 100 % have been assumed for the BSS, in line with typical values reported in the scientific literature [42]. For the alkaline electrolyser (η_{ch}^{H2}), a specific energy consumption of 4.3 kWh/Nm^3 has been considered, corresponding to an efficiency of 70 % based on the lower heating value (LHV) of hydrogen [42,48]. Similarly, the fuel cell efficiency (η_{dis}^{H2}) has been calculated as the ratio of the nominal fuel cell voltage, assumed to be 0.63 V, to the reversible open-circuit voltage of 1.253 V (based on the LHV) [42]. It is important to note that these efficiencies apply specifically to the electrolyser and fuel cell stacks, as the energy consumption of the balance of plant (BoP) and energy conversion stages are accounted for separately in the overall power balance.

For the MPC controller design parameters, typical values for variable, fixed, startup, and degradation costs have been considered for each ESS, in accordance with values commonly reported in the scientific literature [42]. Finally, the operating constraints for the ESS, grid, and state vector have been defined based on safe operating ranges recommended by the manufacturer for both the BSS and the hydrogen tank.

Results and discussion

This section presents and analyses the results obtained from the two hierarchical EMS approaches based on two-level MPC: the economic method (the new approach proposed in this work) and the tracking method. The objective is to validate the performance of the economic method in terms of behaviour, economic benefits, and computational cost compared to the tracking method for three controller settings studied on the microgrid described in the case study. These controller settings are based on CAT I [28,32] (controller setting 1) and CAT III [16,39] (controller setting 2 and 3) solutions. The analysis also explores the impact of the weights and terms in the tracking method's index on the microgrid's response. The validation will be conducted across multiple case studies (scenarios) to assess the performance of the proposed method under varying energy conditions, defined by different generation and demand profiles. Specifically, four scenarios have been

considered: a sunny day with high demand profile (scenario 1), a cloudy day with high demand profile (scenario 2), a sunny winter day with high demand profile (scenario 3), and a cloudy day with low demand profile (scenario 4).

To maintain a manageable manuscript length and given that the analysis and results demonstrate similar microgrid operation across all controllers and scenarios, only the simulation results for scenario 1 are presented and analysed for all controller configurations. The results for the remaining scenarios have been plotted and uploaded to a repository[1] for accessibility, and their economic and computational cost results are summarized in Table 6.

Additionally, these responses are compared to the optimal response obtained by implementing a single-level economic EMS with $PH = PH_{HL}$ and $Ts = Ts_{LL}$. This single-level economic EMS is considered the reference response, as it represents the best possible performance of the microgrid. The optimisation for this reference response follows the methodology outlined in [9], using the same design parameters, costs, constraints, defined losses, model, decision variables, and economic cost function as those used for the HL of the two-level approaches (see Section 4.1). Degradation costs are also included, resulting in the best economic outcome.

However, it is important to note that while this single-level optimisation yields the most favourable economic results, its computational cost is high for real-time applications, making it unsuitable for these applications. In this paper, this procedure is solely for comparison with the two bilevel approaches described.

To demonstrate the feasibility of implementing the compared two-level approaches in real-time, a timeout period equal to Ts_{LL} has been set for each MPC. Thus, if the optimiser fails to find the optimal solution within this time frame, it provides the best sub-optimal solution available at that moment. Additionally, all approaches in this paper include a constraint ensuring that $SOC_j(0) = SOC_j(PH_{HL})$ (see Table 2). This constraint, included in the HL for two-level hierarchical MPC-based EMS maintains consistency between the initial and final EMS levels, preventing any influencing on the economic cost calculations.

The control procedure remains consistent across all bilevel cases studied. The process starts at 8:00 h, when the HL optimiser calculates references, in the first sample time, for a planning horizon (PH_{HL}) and sampling period (Ts_{HL}). These references are used as inputs for the LL optimiser, which operates over the interval 8:00–9:00 h. The LL optimiser applies its first control action ($Ts_{LL} = 30$ sec) and subsequently re-optimises for shorter horizons ($PH_{LL} = 59$min 30sec). This iterative process continues until the hour ends. At 9:00 h, the HL optimiser updates the references, trimming the PH_{HL} to 23 h with $Ts_{HL} = 1$h. This cycle repeats hourly, covering the entire 24-hour period.

Initially, the microgrid's response with the reference EMS is analysed for scenario 1. Fig. 4 shows the results for the single-level MPC-based EMS (optimal EMS). Positive power values indicate energy supplied to the bus, while negative values indicate energy consumption. All power parameters and SOCs meet the constraints defined in Table 2.

The test starts at sunrise (8:00 h), with renewable energy generation producing surplus energy during the first half of the day. This excess energy charges the ESSs (battery and hydrogen tank) and is subsequently sold to the MEG when the battery reaches its SOC limit ($\overline{SOC_{bat}}$), generating economic benefits. At sunset, energy deficits occur, and stored energy is used during high-cost intervals (19:00–23:00 h) as MEG energy prices are higher during these periods (see purchase price in Table 4). To minimize degradation costs, the electrolyser and fuel cell operate at constant power, reducing penalties for power variations.

Once the ESSs reach their minimum levels, energy is purchased during low-cost intervals (e.g., 4:00–5:00 h) to recharge batteries and avoid high-cost purchases later (e.g., 6:00–8:00 h, when energy prices are higher than in the earlier interval), see Table 4. This strategy effectively reduces economic costs.

Finally, Table 6 summarises the economic and computational costs outcomes of this strategy for all scenarios. The approach achieves economic costs of €2.47, €3.06, €5.21, and €1.91 for scenarios 1 to 4, respectively, primarily driven by variable costs. However, the computational time reaches almost 7 min in some scenarios. This makes it impractical, considering that it is a simple microgrid, and real-time applications require a computational cost lower than $Ts_{LL} = 30$ sec.

Next, the results of the EMS tracking approach are analysed for the three predefined controller settings for scenario 1.

Specifically, Fig. 5 presents the results for controller setting 1, where normalized unit weights are used to penalise powers deviations relative to P_i^{ref}. This method avoids the need to define weights in the LL index.

In the first half of the test, there is a continuous cycle of energy purchasing and selling to the MEG, despite an energy surplus during this period. Economically, this is suboptimal as purchasing energy is more expensive than selling it, resulting in an undesired cost. This behaviour arises because the LL index prioritizes strict tracking of reference power variables. For instance, at 9:00 h, the HL provides the following references: $P^{ref}_{ch_{bat}} = 1410$ W, $P^{ref}_{dis_{bat}} = P^{ref}_{ch_{H2}} = P^{ref}_{dis_{H2}} = P^{ref}_{grid_p} = P^{ref}_{grid_s} = 0$ W. The HL determines that the best strategy is to charge the battery using surplus energy. However, at the start of the hour, the actual energy produced by the solar panels is less than predicted (mean). To minimize deviations from $P^{ref}_{ch_{bat}}$, the MPC purchases energy.

Later in the hour, excess energy above the HL's prediction leads the EMS to sell energy to stay aligned with $P^{ref}_{ch_{bat}}$. This pattern repeats in the initial hours, contributing to economic losses.

Additionally, the electrolyser frequently switches on and off during the test. For example, at 11:00 h, the HL provides references indicating that the electrolyser should remain off: $P^{ref}_{dis_{bat}} = 3873.6$ W, $P^{ref}_{ch_{bat}} = P^{ref}_{ch_{H2}} = P^{ref}_{dis_{H2}} = P^{ref}_{grid_p} = P^{ref}_{grid_s} = 0$ W. However, during the interval 11:00–12:00 h, the energy demand fluctuates significantly. Note that during the first part of the interval from 11:00–12:00 h, there is a much lower energy demand ($P_{nMEF-} = 25$ 0 W) than the second part ($P_{nMEF-} = 3750$ W). To minimise deviations, the LL switches on the electrolyser, which has a minimum power of $\underline{P_{ch_{H2}}} = 1000$ W and a balance of plant loss of $Loss_i^{BoP} = 1000$ W, so that the battery charging power does not deviate excessively from the reference. The use of this BoP causes less deviation when switching on the electrolyser compared to any other device. For example, with an excess power of 2000 W, switching on the electrolyser results in a smaller deviation (1000 W from $P_{ch_{H2}}$ and 1000 W from $Loss^{BoP}_{ch_{H2}}$) than using other devices without BoP, which would cause a 2000 W deviation. This explains the frequent electrolyser activation, as seen during the 18:00–19:00 h interval. Once the ESS SOC reaches its maximum, excess energy is sold to the MEG.

In the second half of the test, energy is purchased during low-cost hours (e.g., after 23:00 h) to address energy deficits, as recommended by the HL. However, the electrolyser switches on again briefly (e.g., 1:50–2:00 h) to align with HL references, even when not explicitly suggested. This leads to a final hydrogen storage level slightly higher than the initial level ($SOC_{H_2}(PH_{HL}) = 10.6\%$ vs $SOC_{H_2}(0) = 10\%$).

This microgrid operation, marked by the inefficient use of the HBSS and energy transactions with the MEG under unfavourable conditions, is consistently observed in scenarios 2 to 4 (see scenarios[1]).

Finally, Table 6 summarises the economic and computational costs for this controller setting for all scenarios. All power and SOC variables satisfy the constraints outlined in Table 2. With this controller settings, the optimizer reaches the timeout several times. For example, in the scenario 1, the timeout was reached 800 times. This problem is recurrent and occurs in all the proposed scenarios with this controller setting.

Fig. 6 shows the results for the tracking approach using controller setting 2, with weights defined in Table 5. Overall, the microgrid's

[1] Available in https://riunet.upv.es/handle/10251/219944

Table 6
Economic and computational costs obtained by each approach.

Scenario	Hierarchical two-level MPC-based EMS	Total variable cost* C^{var}	Total fix cost* C^{fix}	Total start cost* C^{Start}	Total degradation cost* C^{deg}	TotalCost	Computational Cost**
1	Optimal	2.31 €	0.060 €	0.10 €	0.000 €	2.47 €	94.13 sec.
Sunny summer day	Tracking (Controller setting 1)	2.85 €	0.066 €	1.05 €	0.120 €	4.08 €	2.05 sec.
High Demand	Tracking (Controller setting 2)	2.73 €	0.060 €	0.10 €	0.000 €	2.89 €	1.61 sec.
	Tracking (Controller setting 3)	2.48 €	0.062 €	0.10 €	0.013 €	2.66 €	2.35 sec.
	Economic	2.37 €	0.06 €	0.10 €	0.000 €	2.53 €	0.79 sec.
2	Optimal	2.90 €	0.055 €	0.10 €	0.000 €	3.06 €	171.54 sec.
Sunny winter day	Tracking (Controller setting 1)	3.58 €	0.060 €	1.60 €	0.170 €	5.41 €	5.9 sec.
High Demand[1]	Tracking (Controller setting 2)	3.12 €	0.159 €	0.20 €	0.002 €	3.48 €	2.64 sec.
	Tracking (Controller setting 3)	3.09 €	0.056 €	0.95 €	0.067 €	4.16 €	3.43 sec.
	Economic	3.02 €	0.050 €	0.10 €	0.000 €	3.17 €	0.82 sec.
3	Optimal	5.10 €	0.012 €	0.10 €	0.000 €	5.21 €	443.77 sec.
Cloudy day	Tracking (Controller setting 1)	6.02 €	0.026 €	1.40 €	0.104 €	7.55 €	9.91 sec.
High Demand[1]	Tracking (Controller setting 2)	5.78 €	0.000 €	0.00 €	0.000 €	5.78 €	2.42 sec.
	Tracking (Controller setting 3)	5.66 €	0.019 €	0.50 €	0.017 €	6.20 €	2.20 sec.
	Economic	5.45 €	0.011 €	0.10 €	0.000 €	5.56 €	0.85 sec.
4	Optimal	1.91 €	0.000 €	0.00 €	0.000 €	1.91 €	49.89 sec.
Cloudy day	Tracking (Controller setting 1)	2.35 €	0.009 €	2.30 €	0.002 €	4.66 €	11.83 sec.
Low Demand[1]	Tracking (Controller setting 2)	2.15 €	0.000 €	0.00 €	0.000 €	2.15 €	2.46 sec.
	Tracking (Controller setting 3)	1.98 €	0.000 €	0.00 €	0.000 €	1.98 €	3.48 sec.
	Economic	1.93 €	0.000 €	0.00 €	0.000 €	1.93 €	0.88 sec.

* $C^{var} = \sum_k \sum_i C_i^{var} \cdot P_i(k) \cdot T_s$, $C^{fix} = \sum_k \sum_i C_i^{fix} \cdot WT_i(k) \cdot T_s$, $C^{Start} = \sum_k \sum_i C_i^{Start} \cdot Start_i(k)$ and $C^{deg} = \sum_k \sum_i C_i^{deg} \cdot \delta P_i^2(k)$.
** Average computational cost of each iteration (CPU processor Intel Core i9, 3.7 GHz with 32 GB RAM).

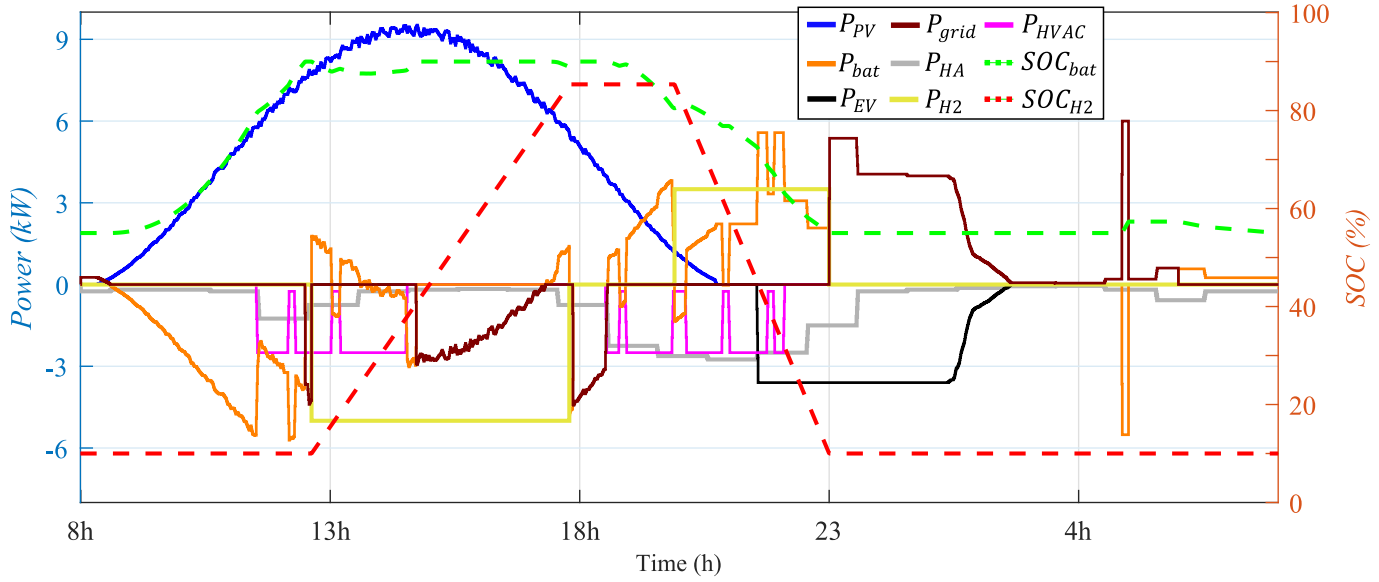

Fig. 4. Power and SOC profiles obtained for residential application for the optimal MPC-based EMS for scenario 1.

behaviour for this controller setting is similar to controller setting 1, where energy purchases and sales to the MEG persist during the first half of the test. This undesired behaviour again stems from minimizing tracking errors relative to HL references. However, controller setting 2 avoids unnecessary electrolyser startups not indicated by the HL. This improvement is due to incorporating startup penalties (ω_{Start_i}), which reduce the frequency of electrolyser activation. As a result, the total start cost ($C^{Start} = \sum_k \sum_i C_i^{Start} \cdot Start_i(k)$) decreases. In addition, avoiding energy purchases from the MEG during intervals such as 1:50–2:00 h reduces the total variable cost ($C^{var} = \sum_k \sum_i C_i^{var} \cdot P_i(k) \cdot T_s$).

This operation uses HBSS more conservatively than the controller setting 1 and remains consistent across all scenarios (see scenarios[1]). As

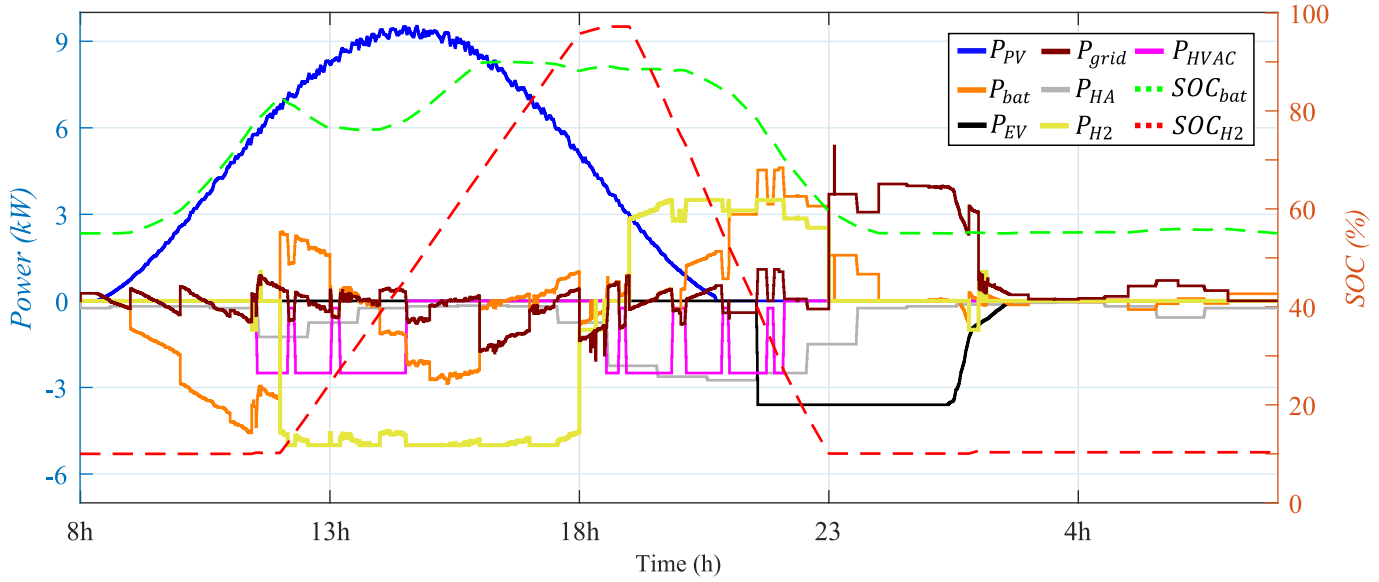

Fig. 5. Power and SOC profiles obtained for residential application for the hierarchical two-level MPC-based EMS tracking for the controller setting 1 for scenario 1.

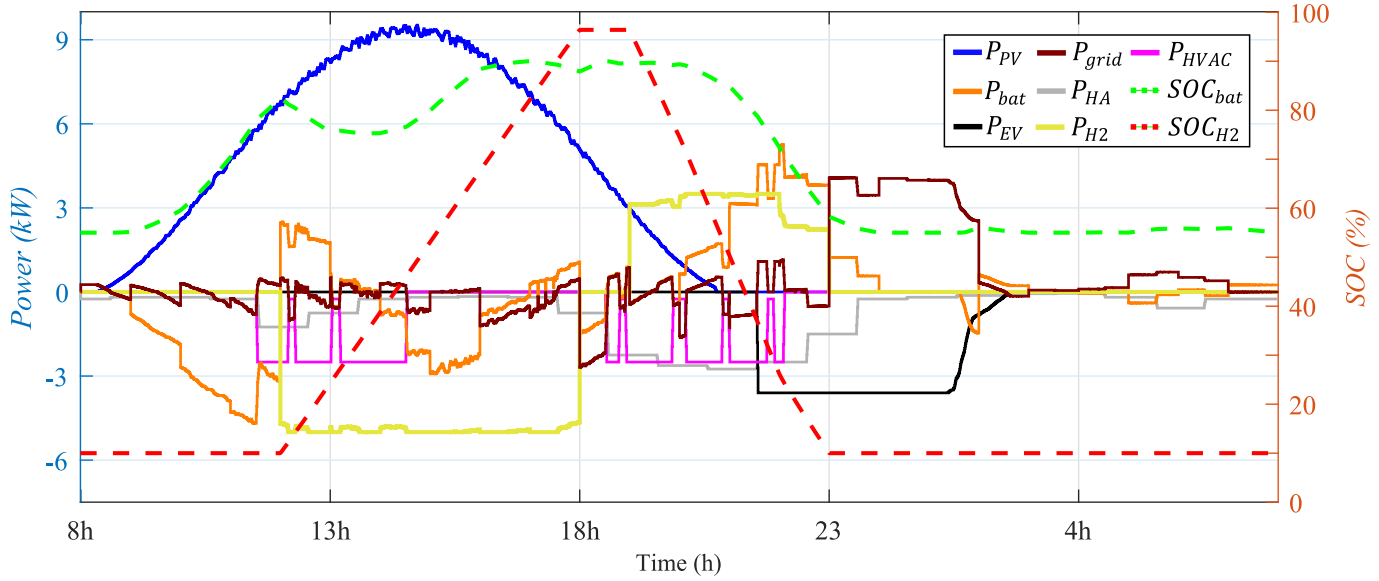

Fig. 6. Power and SOC profiles obtained for residential application for the hierarchical two-level MPC-based EMS tracking for the controller setting 2 for scenario 1.

a result, it reduces costs by more than 23 % compared to the previous setting in all case studies. The economic and computational costs for all scenarios are detailed in Table 6. Once again, while all power and SOC variables satisfy the constraints specified in Table 2, the optimiser reaches the timeout limit in several iterations. In the scenario 1, the timeout was reached 250 times. This problem occurs in all the proposed scenarios with this controller setting.

Fig. 7 presents the results for controller setting 3, with weights also defined in Table 5. This controller setting achieves a more efficient use of the MEG and a more stable operation of the HBSS.

Notably, energy purchases and sales to the MEG are eliminated in the first half of the test, thanks to higher penalties for deviations in MEG power. This reduces the total variable cost by minimizing energy purchases. Additionally, electrolyser startups are avoided by applying ω_{Start_i}, while HBSS power is stabilized, reducing power fluctuations and the total degradation cost.

As in previous cases, the microgrid operation remains consistent across all scenarios (see scenarios[1]). This leads to a cost reduction up to 8 % compared to controller setting 2 in all case studies. Table 6 summarises the economic and computational cost for all scenarios. The optimiser reaches the timeout limit in 48 times in the scenario 1. Again, this problem is recurrent in all the proposed scenarios. All power and SOC constraints specified in Table 2 are satisfying.

Finally, Fig. 8 shows the results of the proposed MPC-based economic EMS. The economic and computational costs are seen in Table 6. All power parameters and SOCs meet the constraints defined in Table 2. As for controller setting 3, undesired energy purchases and sales during periods of excess power are avoided. Between 9:00–17:45 h MEG power in nearly zero. This approach optimises the use of the HBSS and MEG, enabling increased H2 production and reducing reliance on MEG energy purchases. This leads to improved cost efficiency compared to previous controller settings.

For instance, in the prior controller setting, energy was purchased between 1:00–2:00 h to avoid higher-cost purchases during 2:00–3:00 h

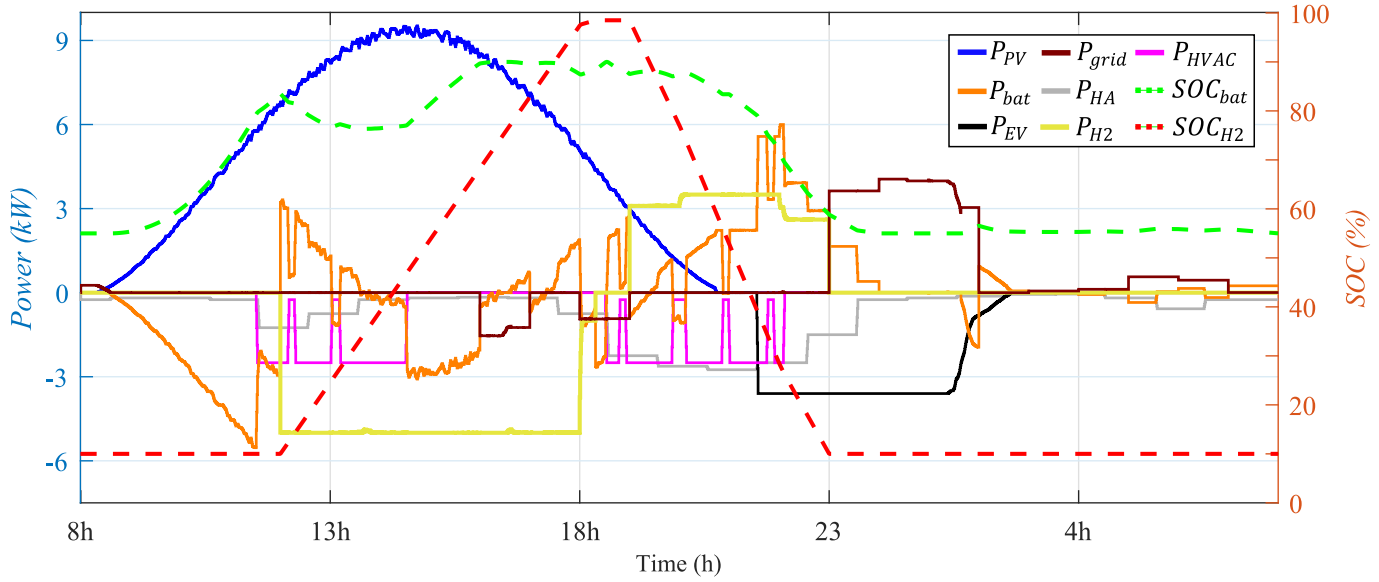

Fig. 7. Power and SOC profiles obtained for residential application for the hierarchical two-level MPC-based EMS tracking for the controller setting 3 for scenario 1.

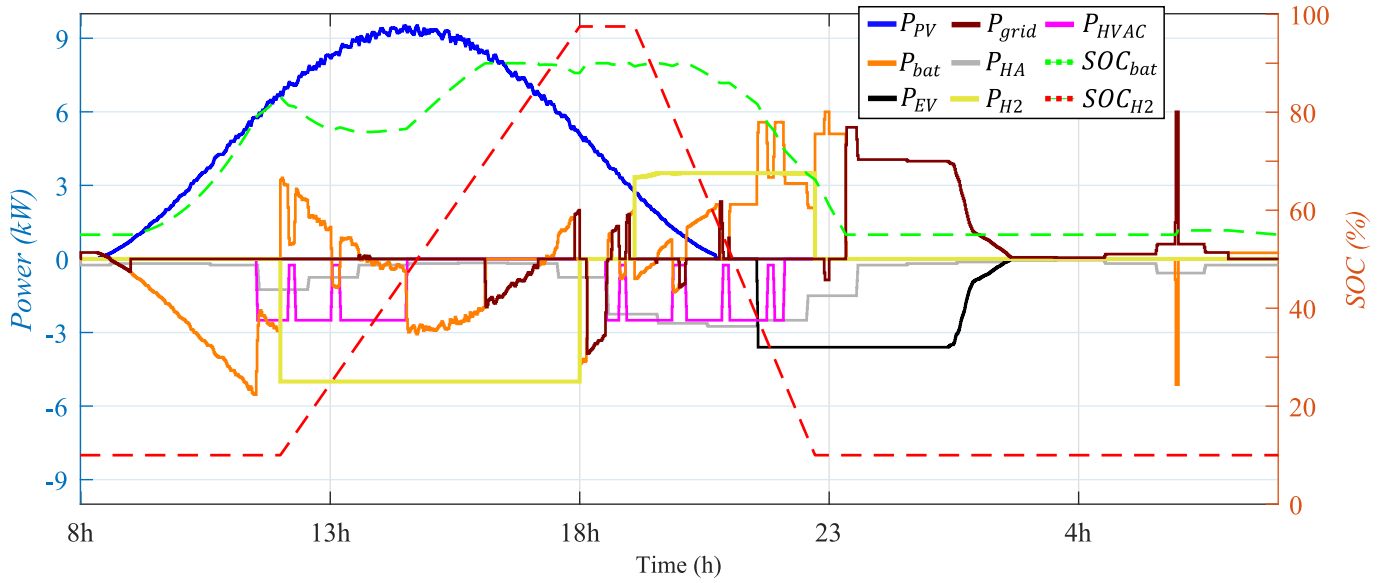

Fig. 8. Power and SOC profiles obtained for residential application for the new two-level MPC-based EMS economic for scenario 1.

and 7:00–8:00 h. However, 1:00–2:00 h was not the most cost-effective time slot. In contrast, the economic EMS approach shifts energy purchases to the 5:00–6:00 h interval, which has lower costs, thereby avoiding purchases during the expensive 7:00–8:00 h period. This adjustment results in reduced total variable costs (refer to Table 6, scenario 1).

Additionally, the economic EMS approach significantly improves HBSS management by ensuring the electrolyser and fuel cell operate with a stable power profile. This stability minimizes the total degradation cost ($C^{deg} = \sum_k \sum_i C_i^{deg} \cdot \delta P_i^2(k)$). Additionally, the HBSS operates at maximum power, which reduces its operating time (by 24 min) and cuts the total fixed costs ($C^{fix} = \sum_k \sum_i C_i^{fix} \cdot WT_i(k) \cdot T_s$). In terms of real-time feasibility, this approach has a lower average computational cost per iteration, as shown in Table 6.

Additionally, no iterations exceeded the timeout limit in none of the proposed scenarios, while all power parameters and SOCs meet the constraints defined in Table 2. Once again, the proposed economic MPC approach demonstrates consistent microgrid operation across all studied scenarios (see Table 6 and scenarios[1]). It achieves an economic cost closest to the reference case while significantly reducing computational demands compared to the tracking approach.

Considering the architecture of the microgrid under study, it is interesting to evaluate behaviour of the state variable V_{BUS}. As shown in Fig. 9, V_{BUS} shows consistent behaviour across all controller settings and approaches for scenario 1. Despite instantaneous fluctuations in bus power, V_{BUS} remained within the defined constraints (330–450 V). Once again, this behaviour is reproduced in the rest of the scenarios for all the controller approaches (see scenarios[1]). This demonstrates that the MPC approach is effective for controlling this type of microgrid architecture.

Finally, the results for all scenarios highlight some undesirable behaviours in the MPC tracking approach: (1) constant buying and selling of energy with the MEG, and (2) unnecessary switching on of the electrolyser and fuel cell, which increases costs. These issues can be mitigated by carefully selecting weights, but defining multiple weights can

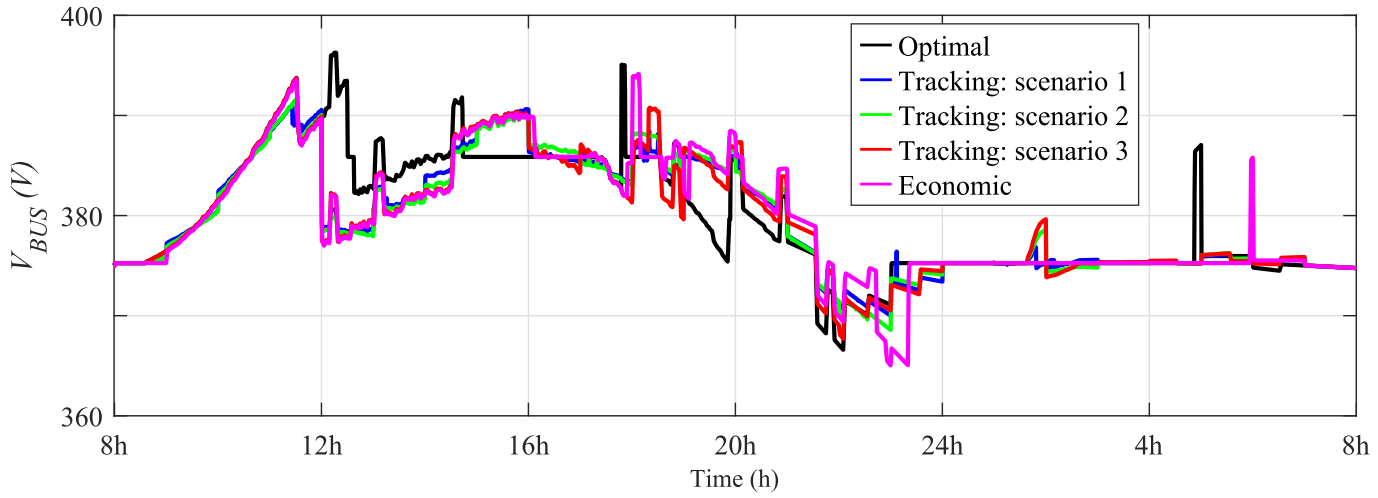

Fig. 9. V_{BUS} profiles obtained for residential application for all approaches and controller settings for scenario 1.

be complex and often requires trial and error, leading to suboptimal solutions. Moreover, these weights are specific to a particular microgrid and need to be adjusted if the microgrid changes.

Furthermore, based on the analysis of all scenarios (see Table 6 and scenarios[1]), the behaviour of the controller settings is not always the same. Thus, controller setting 3 produces the best performance in scenario 1 with tracking approach. However, this is not the case in all scenarios (scenario 2 and 3, where controller setting 2 achieves a lower economic cost). This is due to undesirable behaviours (e.g., restrictive or untimely use of the H2 system) for different situations. This can mitigate by increasing the weight to penalise the number of startups of these devices. However, this increase implies that these devices will not be switched on in other scenarios where it is profitable. Consequently, a given controller setting does not guarantee effective behaviour for all possible scenarios (sunny day, cloudy day, low demand, etc.). Therefore, the controller tuning must be chosen not only for each microgrid, but also for each scenario.

In contrast, the economic approach avoids these undesired effects, eliminates the need for trial-and-error weight selection, and consistently delivers better economic outcomes than the tracking approach. Thus, the proposed two-level economic MPC approach, as described in Sections 2 and 3, proves to be an effective tool for real-time microgrid management, irrespective of its architecture or topology.

Finally, despite the excellent results demonstrated by the proposed MPC-based EMS with a two-level hierarchical structure, its real-time implementation in large grids with numerous constraints and uncertainties presents significant computational challenges. As shown in the paper, for a microgrid of considerable complexity, computation times may not be compatible with real-time applications.

Nevertheless, several strategies could be explored to address these computational challenges. These include parallelizing the problem, implementing a dynamic prediction horizon based on network dynamics, utilizing a high-performance computing system (as this study employed a general-purpose computer), or, as a last resort, simplifying the problem by relaxing certain constraints.

It is important to note that optimizing the computational efficiency of the developed techniques was not the primary objective of this work.

Conclusions

This paper presents a novel MPC-based EMS with a two-level hierarchical structure to optimize microgrid control. The literature has amply demonstrated that MPC-based EMSs are efficient and cost-effective strategies. In a hierarchical control architecture, HL optimizes long-term economic management, which requires appropriately defining the economic costs of each device. However, the control strategy of the LL is not trivial. This study compares two hierarchical MPC-based EMS approaches with different LL strategies: the traditional tracking-based method and a proposed economic optimization approach.

The analysis shows that the tracking-based approach has limitations that can affect system performance, such as:

1.- Unnecessary energy transactions: The LL attempts to minimize deviations from the references imposed by the HL, which leads to constant energy purchases and sales. This situation arises from the difference between the long-term energy predictions of the HL and the shorter sampling intervals of the LL.

2.- Frequent device switching: The LL repeatedly switches on and off equipment, such as electrolysers, to adjust to the HL references, especially based on Balance of Plant (BoP) requirements. This frequency switching accelerates the wear of critical components, such as hydrogen systems.

These problems can be mitigated by manually adjusting the settings controller. However, this process is based on trial and error, lacks a physical interpretation, and highly depends on each microgrid and scenario (e.g., weather conditions and energy demands). As a result, any change to the system or scenario requires redefining controller settings parameters to avoid economic losses or premature equipment wear.

In contrast, the economic MPC-based EMS approach addresses these shortcomings in all the scenarios analysed. This method avoids unnecessary energy transactions and excessive device switching while eliminating the need for manual weight adjustment. Furthermore, it relies on the economic costs already defined in the HL, which (1) ensures greater consistency and stability in the control strategy and (2) avoids the definition of physically meaningless weights through trial and error.

The results demonstrate that the proposed economic approach reduces operating costs by 3 % to 58 % compared to the tracking method, achieving values close to single-level optimal control. Consequently, economic MPC is an efficient and robust solution for microgrid management. However, a potential limitation of the proposed approach was identified: in certain cases, the LL may not meet the final equality constraint within the prediction horizon, leading to infeasible solutions. This issue should be addressed in future work.

Future research will focus on implementing the method in real-time microgrids and developing advanced optimal control strategies for dynamic environments. The integration of uncertainties and disturbances into the model, predictions, and controller parameterization will also be explored to improve their applicability in real-world scenarios.

Another line of future research concerns the application of the developed MPC-based EMS with a two-level hierarchical structure in

situations where the control problem is too computationally demanding (large grids with numerous constraints and uncertainties). Alternative solutions could be explored here, such as simplifying the problem, using additional control levels or investigating other control strategies aimed at reducing computational costs, such as move-blocking or variable horizon strategies. These approaches will be the subject of future work by the authors.

CRediT authorship contribution statement

F.J. Vivas: Writing – original draft, Methodology, Investigation, Conceptualization. **A. Pajares:** Writing – original draft, Software, Methodology, Investigation, Conceptualization. **X. Blasco:** Writing – review & editing, Supervision, Project administration, Investigation. **J. M. Herrero:** Writing – review & editing, Supervision, Project administration, Investigation, Conceptualization. **F. Segura:** Writing – review & editing, Supervision, Project administration, Funding acquisition. **J.M. Andújar:** Writing – review & editing, Writing – original draft, Supervision, Project administration, Funding acquisition.

Declaration of competing interest

The authors declare that they have no known competing financial interests or personal relationships that could have appeared to influence the work reported in this paper.

Acknowledgements

This work has been funded by project PID2023-148456OB-C41, funded by MICIU/AEI/10.13039/501100011033 and FEDER, EU. Also to be mentioned is the participation of the Valencian regional government in 'ERDF A way of making Europe' through project CIAICO/2021/064.

Data availability

No data was used for the research described in the article.

References

[1] Vivas FJ, De las Heras A, Segura F, Andújar JM. A review of energy management strategies for renewable hybrid energy systems with hydrogen backup. Renewable and Sustainable Energy Rev 2018;82:126–55.
[2] Garcia-Torres F, Zafra-Cabeza A, Silva C, Grieu S, Darure T, Estanqueiro A. Model predictive control for microgrid functionalities: review and future challenges. Energies 2021;14(5):1296.
[3] Hajiaghasi S, Salemnia A, Hamzeh M. Hybrid energy storage system for microgrids applications: A review, *J Energy Storage*, 21 (November 2018), 543–570, 2019.
[4] Monforti Ferrario A, et al. A model-based parametric and optimal sizing of a battery/hydrogen storage of a real hybrid microgrid supplying a residential load: Towards island operation. *Adv Appl Energy* 2021;3(June):100048.
[5] Dekkiche M, Tahri T, Denai M. Techno-economic comparative study of grid-connected PV/reformer/FC hybrid systems with distinct solar tracking systems, *Energy Convers Manage: X*, vol. 18, no. December 2022, p. 100360, 2023.
[6] Abbasi AR, Baleanu D. Recent developments of energy management strategies in microgrids: An updated and comprehensive review and classification. *Energ Conver Manage* 2023;297(October):117723.
[7] Vivas Fernández FJ, Manzano FS, Márquez JMA, Calderón Godoy AJ. Extended model predictive controller to develop energy management systems in renewable source-based smart microgrids with hydrogen as backup. Theoretical foundation and case study. *Sustainability (switzerland)* 2020;12(21):1–28.
[8] He Y, Li Z, Zhang J, Shi G, Cao W. Day-ahead and intraday multi-time scale microgrid scheduling based on light robustness and MPC. *Int J Electr Power Energy Syst* 2022;144(July):2023.
[9] Pajares A, Vivas FJ, Blasco X, Herrero JM, Segura F, Andújar JM. Methodology for energy management strategies design based on predictive control techniques for smart grids. *Appl Energy* 2023;351(August):121809.
[10] Zhang J, et al. Multi-time scale economic scheduling method based on day-ahead robust optimization and intraday MPC rolling optimization for microgrid. *IEEE Access* 2021;9:140315–24.
[11] Calderón AJ, Vivas FJ, F. Segura, J. M. Andújar, Integration of a multi-stack fuel cell system in microgrids: A solution based on model predictive control, *Energies*, 13 (18), 2020.
[12] Mbungu NT, Ismail AA, AlShabi M, Bansal RC, Elnady A, Hamid AK. Control and estimation techniques applied to smart microgrids: A review. *Renew Sustain Energy Rev* 2023;179(January):113251.
[13] Holtwerth A, Xhonneux A, Müller D. Closed loop model predictive control of a hybrid battery-hydrogen energy storage system using mixed-integer linear programming. *Energy Convers Manage: X* 2024;22(March).
[14] Zhang L, et al. Hybrid electrochemical energy storage systems: An overview for smart grid and electrified vehicle applications. *Renew Sustain Energy Rev* 2021;139 (November 2020):110581.
[15] Nawaz A, Wu J, Ye J, Dong Y, Long C. Distributed MPC-based energy scheduling for islanded multi-microgrid considering battery degradation and cyclic life deterioration. *Appl Energy* 2023;329(July 2022):120168.
[16] Garcia-Torres F, Bordons C. Optimal economical schedule of hydrogen-based microgrids with hybrid storage using model predictive control. *IEEE Trans Ind Electron* 2015;62(8):5195–207.
[17] Liu C, Wang C, Yin Y, Yang P, Jiang H. Bi-level dispatch and control strategy based on model predictive control for community integrated energy system considering dynamic response performance. *Appl Energy* 2022;310(December):118641.
[18] Huang C, et al. Economic and resilient operation of hydrogen-based microgrids: An improved MPC-based optimal scheduling scheme considering security constraints of hydrogen facilities. *Appl Energy* 2023;335(January):120762.
[19] Beus M, Banis F, Pandžić H, Poulsen NK. Three-level hierarchical microgrid control—model development and laboratory implementation. *Electr Pow Syst Res* 2020;189(April).
[20] Valverde L, Rosa F, Bordons C, Guerra J. Energy management strategies in hydrogen smart-grids: a laboratory experience. *Int J Hydrogen Energy* 2016;41(31): 13715–25.
[21] Bianco G, Delfino F, G. Ferro, M. Robba, M. Rossi, A hierarchical Building Management System for temperature's optimal control and electric vehicles' integration, *Energy Conversion and Management: X*, vol. 17, no. November 2022, p. 100339, 2023.
[22] Yang H, Pu Y, Qiu Y, Li Q, Chen W. Multi-time scale integration of robust optimization with MPC for islanded hydrogen-based microgrid. In: iSPEC 2019–2019 IEEE Sustainable Power and Energy Conference: Grid Modernization for Energy Revolution; 2019. p. 1163–8.
[23] Chang W, Dong W, Wang Y, Yang Q. Two-stage coordinated operation framework for virtual power plant with aggregated multi-stakeholder microgrids in a deregulated electricity market. *Renew Energy* 2022;199(July):943–56.
[24] Wei B, Han X, C. Ren, B. Zhang, Two-Stage Optimal Dispatch for AC/DC Hybrid Microgrid Based on Model Predictive Control, *5th IEEE Conference on Energy Internet and Energy System Integration: Energy Internet for Carbon Neutrality, EI2 2021*, pp. 267–271, 2021.
[25] Bustos R, Marín LG, Navas-Fonseca A, Reyes-Chamorro L, Sáez D. Hierarchical energy management system for multi-microgrid coordination with demand-side management. *Appl Energy* 2023;342(April):121145.
[26] Rashidi R, Hatami A, Abedini M. Multi-microgrid energy management through tertiary-level control: Structure and case study. *Sustainable Energy Technol Assess* 2021;47(January).
[27] Brahmia I, Wang J, de Oliveira L, Xu H. Hierarchical smart energy management strategy based on cooperative distributed economic model predictive control for multi-microgrids systems. *Int Trans Electr Energy Syst* 2021;31(2):1–19.
[28] Lei X, Huang T, Yang Y, Fang Y, Wang P. A bi-layer multi-time coordination method for optimal generation and reserve schedule and dispatch of a grid-connected microgrid. *IEEE Access* 2019;7:44010–20.
[29] Garcia-Torres F, Valverde L, Bordons C. Optimal load sharing of hydrogen-based microgrids with hybrid storage using model-predictive control. *IEEE Trans Ind Electron* 2016;63(8):4919–28.
[30] Kaya O, Van Der Roest E, D. Vries, T. Keviczky, Hierarchical model predictive control for energy management of power-to-X systems, *IEEE PES Innovative Smart Grid Technologies Conference Europe*, vol. 2020-Octob, pp. 1094–1098, 2020.
[31] Zhu Y, Wang J, Bi K, Sun Q, Zong Y, Zong C. Energy optimal dispatch of the data center microgrid based on stochastic model predictive control. *Front Energy Res* 2022;10(March):1–9.
[32] Berkel F, Görges D, Liu S. Load-frequency control, economic dispatch and unit commitment in smart microgrids based on hierarchical model predictive control. In: *Proceedings of the IEEE Conference on Decision and Control*; 2013. p. 2326–33.
[33] Garcia-Torres F, Bordons C, Tobajas J, Real-Calvo R, Santiago I, Grieu S. Stochastic optimization of microgrids with hybrid energy storage systems for grid flexibility services considering energy forecast uncertainties. *IEEE Trans Power Syst* 2021;36 (6):5537–47.
[34] Cominesi SR, Farina M, Giulioni L, Picasso B, Scattolini R. A two-layer stochastic model predictive control scheme for microgrids. *IEEE Trans Control Syst Technol* 2018;26(1):1–13.
[35] Yassuda Yamashita D, Vechiu I, Gaubert JP. Two-level hierarchical model predictive control with an optimised cost function for energy management in building microgrids. *Appl Energy* 2021;285(November 2020):116420.
[36] Hou J, Yu W, Xu Z, Ge Q, Li Z, Meng Y. Multi-time scale optimization scheduling of microgrid considering source and load uncertainty. *Electr Pow Syst Res* 2023;216 (October 2022):109037.
[37] Cheng Z, Jia D, Li Z, Xu S, Zhi C, Wu L. Multi-time scale energy management of microgrid considering the uncertainties in both supply and demand. *Energy Rep* 2022;8:10372–84.
[38] Abdelghany MB, Mariani V, Liuzza D, Glielmo L. Hierarchical model predictive control for islanded and grid-connected microgrids with wind generation and hydrogen energy storage systems. *Int J Hydrogen Energy* 2024;51:595–610.

[39] Garcia-Torres F, Valverde L, Bordons C. Optimal load sharing of hydrogen-based microgrids with hybrid storage using model-predictive control. *IEEE Trans Ind Electron* 2016;63(8):4919–28.
[40] Vivas FJ, Segura F, Andújar JM, Calderón AJ, Isorna F. Battery-based storage systems in high voltage-DC bus microgrids. A real-time charging algorithm to improve the microgrid performance. *J Storage Mater* 2022;48(December):2021.
[41] Vivas FJ, et al. Multi-objective fuzzy logic-based energy management system for microgrids with battery and hydrogen energy storage system. *Electronics (switzerland)* 2020;9(7):1–25.
[42] Bordons C, Garcia-Torres F, Ridao MA. Model Predictive Control of Microgrids; 2020.
[43] Roy A *et al.*, A combined optimization of the sizing and the energy management of an industrial multi-energy microgrid: Application to a harbour area, *Energy Convers Manage: X*, vol. 12, no. July, p. 100107, 2021.
[44] Adedoja OS, Sadiku ER, Hamam Y. A techno-economic assessment of the viability of a photovoltaic-wind-battery storage-hydrogen energy system for electrifying primary healthcare centre in Sub-Saharan Africa, *Energy Convers Manage: X*, 23 (May), p. 100643, 2024.
[45] Naderi E, Bibek KC, Ansari M, Asrari A. Experimental validation of a hybrid storage framework to cope with fluctuating power of hybrid renewable energy-based systems. *IEEE Trans Energy Convers* 2021;36(3):1991–2001.
[46] Bemporad A, Morari M. Control of systems integrating logic, dynamics, and constraints. *Automatica* 1999;35(3):407–27.
[47] Mignone D, Bemporad A, Morari M. Framework for control, fault detection, state estimation, and verification of hybrid systems. In: *Proceedings of the American Control Conference*; 1999. p. 134–8.
[48] Carmo M, Fritz DL, Mergel J, Stolten D. A comprehensive review on PEM water electrolysis. *Int J Hydrogen Energy* 2013;38(12):4901–34.